Biomass gasification processes - modeling and simulation

Pedro Afonso Fatori Maldonado

Final dissertation report submitted to the Escola Superior de Tecnologia e Gestão of the Instituto Politécnico de Bragança to obtain the Master´s Degree in Chemical Engineering in the scope of the double diploma with the Universidade Tecnológica Federal do Paraná - Ponta Grossa

Supervisors

Prof. Dr. Paulo Miguel Pereira de Brito
Prof. Dr. Helder Teixeira Gomes
Prof. Dr. Giane Gonçalves Lenzi

Bragança
October, 2022

Acknowledgments

Firstly, I would like to thank my grandmother Ambrosina who participated in almost all my growth, and helped me to reach where I am, and to be who I am. Thanks, mom, brother, uncles, and people of my family to believe in me and supporting me all this time, I love you. I thank my supervisors Prof. Paulo Brito, Prof. Helder Teixeira, and my co-supervisor Prof.ª Giane Lenzi to provide me with all knowledge, tools, and orientation, and for being always patient and pleasant. Thanks, Universidade Tecnológica Federal do Paraná - Ponta Grossa, professors, and collaborators, which afforded me the knowledge necessary to be here and do this, worth mentioning the free public education guaranteed by the government. Thanks, Instituto Politénico de Bragança - Bragança, professors, and collaborators to welcome me and for making this aim possible. This work is still assisted by the Portuguese Foundation of Science and Technology (FCT) within the framework of the SUBe Project. Thank you, canteen workers, to make me part of the family and help me in times of necessity. Last, but not least, my friends in my city Ilha Solteira, or made through the University in Ponta Grossa. My friends who came with me to Bragança, and the ones that I knew here. I will not name names, but I carry in my heart each moment that spent with you, good or bad, and each support that you gave to me, helping me to improve as a person, and keeping my soul alive. You are part of this achievement. Thank you all.

Abstract

Thermochemical processes prove to be a sustainable way of using residual biomass, replacing non-renewable sources such as coal and petroleum derivatives, and serving as a means for the creation of Synthesis Gas, or Syngas, mostly consisting of hydrogen gas and carbon monoxide, which is the basis for the chemical industry and power generation. The modeling and simulation of this process is feasible, as it portrays real gasifiers, such as Downdraft type gasifiers, in order to test variables and verify the system's behaviors when changing them. However, there is still some difficulty in modeling Pyrolysis, due to the complexity of this process, as well as predicting the tar generated during the process. Thus, the present study aims to model and simulate using the UniSim Design software, the gasification of three biomass residues from Portuguese agriculture: grape marc, olive trees, and corn straw residues, in an attempt to predict Syngas production under different process conditions and validate the method proposed comparing with data from the literature. Pyrolysis modeling was performed using a second-order model based on the process temperature, providing the yields of gases: CO_2, CO, H_2, and CH_4, residual coal, and tar, which is composed of benzene, toluene, and naphthalene. Regarding the results obtained, both Pyrolysis and the general model, even at different conditions of mass flow of air and steam inlet, were compatible with results obtained in the literature, quantitatively and qualitatively. The rise in equivalence ratio (ER) from 0.23 to 0.54 caused an increase in the process temperature, as well as in the molar fraction of H_2 and CO while reducing the other components, thus consuming the tar, for the biomasses in the ER range 0.36-0.37. The increase in the steam-to-biomass ratio (S/B) from 0 to 0.95 had a positive effect on the H_2 and CO_2 components, while it decreased the others, having no effect on the tar fraction. For both analyses, corn straw residue was converted into the richest gas in hydrogen, with the peak of the fraction of the component in Syngas, free of water and nitrogen, being 0.48 and 0.52, for ER and S/B ratio, respectively.

Keywords: Biomass gasification; Pyrolysis process; Downdraft gasifier; Syngas; Simulation; UniSim Design.

Resumo

Processos termoquímicos mostram-se uma forma sustentável de utilizar biomassas residuais, substituindo fontes não renováveis como carvão e derivados de petróleo, e servindo de meio para a criação do Gás de síntese, ou Syngas, majoritariamente constituído por gás hidrogênio e monóxido de carbono, o qual é uma base para a indústria química e geração de energia. A modelagem e simulação deste processo é viável, pois retrata gaseificadores reais, como o gaseificador do tipo Downdraft, a fim de testar variáveis e verificar os comportamentos do sistema ao alterá-las. Porém, ainda há certa dificuldade na modelagem da Pirólise, devido à complexidade deste processo, bem como a previsão da produção do alcatrão gerado durante o processo. Desta forma, o presente estudo tem por objetivo modelar, e simular no software UniSim Design a gaseificação de três resíduos provindos da agricultura portuguesa: resíduos de uva, oliveiras e milho, na tentativa de predizer Syngas sob diferentes condições de processo e validar o método proposto por comparação com dados da literatura. A modelação da Pirólise foi realizada utilizando um modelo de segunda ordem baseado na temperatura do processo, provendo os rendimentos dos gases: CO_2, CO, H_2 e CH_4, do carvão residual e do alcatrão, o qual é composto por benzeno, tolueno e naftaleno. Acerca dos resultados obtidos, tanto a Pirólise, quanto o modelo geral, mesmo a diferentes condições de fluxo mássico de entrada de ar e vapor, mostraram-se compatíveis com resultados obtidos na literatura, quantitativamente e qualitativamente. O aumento no ER de 0,23 até 0,54 provocou um aumento na temperatura do processo, bem como da fração molar de H_2 e CO, enquanto reduziu os demais componentes, consumindo o alcatrão para as biomassas na faixa de ER 0,36-0,37. O incremento da razão S/B de 0 a 0,95 provocou um efeito positivo nos componentes H_2 e CO_2, enquanto decresceu os demais, não tendo efeito na fração do alcatrão. Para ambas as análises, o resíduo de milho converteu-se no gás mais rico em hidrogênio, sendo o pico da fração do componente no Syngas, livre de água e nitrogênio, 0,48 e 0,52, para ER e razão S/B, respectivamente.

Palavras-chave: Gaseificação de biomassa; Processo de Pirólise; Gaseificador Downdraft; Syngas; Simulação; UniSim Design.

LIST OF FIGURES

LIST OF TABLES

LIST OF ACRONYMS

ASH - Ash

CCE - Carbon conversion efficiency

CGE - Cold gas efficiency

CFD - Computacional fluid dynamic

CS - Corn straw

EM - Equilibrium model

ER - Equivalence ratio: $(air/fuel)_{actual}/(air/fuel)_{stoichiometric}$

FC - Fixed carbon

GM - Grape marc

HHV - Higher Heating Value (MJ/Nm^3)

H/C - Hydrogen-carbon ratio

KM - Kinetic model

LHV - Lower Heating Value (MJ/Nm^3)

M - Moisture

O/C - Oxygen-carbon ratio

OR - Olive residue

PA - Proximate analysis

S/B ratio - Steam to biomass ratio

Syngas - Synthesis gas

UA - Ultimate analysis

VM - Volatile matter

TABLE OF CONTENTS

1 MOTIVATION

In all countries, energy is the solution to many problems, like the primary needs of the population, industrial movement, and maintenance of cities in general, however, the way to reach it has been harmful to the environment. For many years, oil derivates, natural coal, and natural gas were used, and still are, as primary energy supply due to their calorific potential, and their great available amount on the earth. It is common fact that the utilization of these feedstocks causes greenhouse effects and helped in global warming, creating a general concern about this issue, and leading to the creation of urgent measures to get around.

Based on it, guidelines and public policies were granted by European Union, to guarantee the reduction of emissions and increase the portion of renewable sources in energy system production. An example is the Portuguese Decree-Law n.152-C/2017, issued by the European Directive, which promotes the energy production and use of biofuels from waste, forest biomass as its waste, human and animal food waste, algae, and cellulosic biomass, or subproducts derived from agricultural food species, like straw, stover, husks, and shells [1].

The main sources of primary energy in Portugal are oil, coal, and natural gas, making the country dependent on importations of resources, due to the absence of oil reserves [2]. Besides, more than 85% of the country is covered by vegetation (39% by forest, 26.3% by agricultural land, 12.4 by bush, and 8% by agroforestry systems) [1], representing another possibility for energy-producing. Biomass rich in sugar like sugarcane, corn, and wheat, or rich in oil, such as soil beans, coconut, palm, and olives can be converted into biofuels by biochemical processes, though it, sometimes, can cause a conflict between food and fuels [1].

Thermochemical processes convert biomasses into energy or fuels with a high heating value through high-temperature treatments. It comprises Combustion, Pyrolysis, Gasification, Torrefaction and Liquefaction, which can be employed together or separated, depending on the need. The gasification product is Synthesis Gas, comprehended mainly by hydrogen gas (H_2) and carbon monoxide (CO), which can be used posteriorly to produce electric energy. In this process, many parameters such as temperature, pressure, gasifying agent, biomass composition (main structures, Cellulose, Hemicellulose, Lignin), gasifier, and others, influence the final composition of the gas.

Agricultural residues by cultivation and handling are an important source of lignocellulosic biomass with energetic potential that can be fed in thermochemical processes. In Portugal, there is an important production of olive culture, cereal grains, vineyards, and

almonds [2]. Attached to this, these residues have a neutral balance in CO_2 emissions due to the gas absorption during the production of the biomass sources.

A challenge to show the feasibility of Syngas production is trying to know the conversion yields and their composition to evaluate the efficiency of the process. Simulating Software helps in this task, bringing virtual processes closer to real ones. Through Honeywell UniSim Design software, the work intends to create and simulate an Equilibrium model able to predict the lignocellulosic biomass gasification products for Downdraft gasifier, using different sources such as olive and corn straw agricultural wastes, and grape bagasse residue from wine culture.

1.1 Objectives

- Create and simulate biomass gasification models in UniSim Design using specific Pyrolysis modeling strategies based on the literature;
- Simulate olive residue, corn straw, and grape marc wastes using a Downdraft flow gasifier;
- Predict the Syngas compositions in diverse operation conditions;
- Analyze quantitatively and qualitatively the gas produced, varying ER and S/B ratio;
- Validate the process, based on the available literature data.

2 STATE OF THE ART

2.1 Biomass

Biomass is a complex organic-inorganic structure, non-fossilized and biodegradable matter [3] formed in a natural and anthropogenic way, or via human or animal excretion [4]. Biomass sources are shown in Table 1.

Table 1. Biomass sources and subdivisions.

Sources of biomass	Subdivisions.
Agricultural	Food grain; Bagasse; Corn stalks; Straw; Seed hulls; Nutshells; Manure from cattle, poultry, and pigs
Forest	Trees; Wood waste; Wood or bark; Timber slash; Mill scrap
Municipal	Sewage sludge; Refuse-derived fuel; Food waste; Waste paper; Yard clippings
Energy	Poplars willows; Switchgrass; Alfafa; Prairie bluestem; Corn; Soybean; Canola
Biological	Animal waste; Aquatic species; Biological waste

Source. Adapted from [3]

A large part of chemical products that accrue from petroleum and natural gas can be produced from biomass. It is a good way to substitute fossil fuels for energy conversion due to the neutral balance of carbon dioxide (CO_2), which is absorbed by the biomass during the photosynthesis process and is eliminated by the use of biomass in thermochemical processes, not adding more gas to the atmosphere, and not getting worse the greenhouse effect [4].

Some biomass products are charcoal, torrefied biomass, biocoke, and biochar as solid fuels; ethanol, biodiesel, methanol, vegetable oil, and pyrolysis oil, as liquid fuels; biogas, producer gas, and Synthesis Gas or Syngas, as gaseous fuels [5]. Biosyngas, the crude Syngas, is mainly constituted of hydrogen gas (H_2) and carbon monoxide (CO) and can be transformed into many products as shown below in Figure 1.

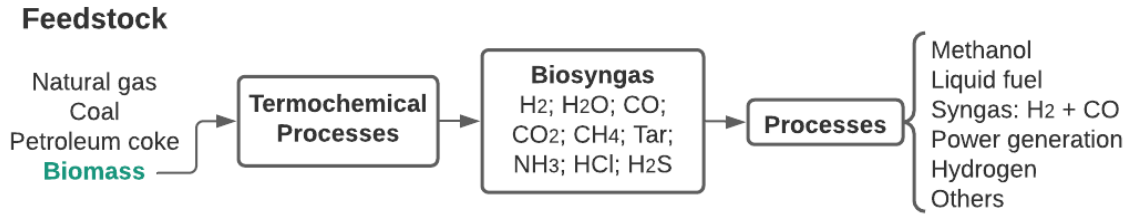

Figure 1. Biomass as Biosyngas source.

2.1.1 Cellulose, Lignin, and Hemicellulose

The organic portion is mostly composed of cellulose, hemicellulose, lignin, and organic minerals, and the inorganic is composed of minerals from phosphates, carbonates, silicates, chlorides, sulfates, nitrates, and others [4].

Cellulose is an organic and crystalline polymer, present in cell walls in biomass [5], composed of at least ten thousand monomers of β-D-glucose [6]. It is the most organic compound on earth and is present between 33-44 wt% for most plants [3]. Lignin maintains the fibers of the plant together [5] and generally is a fraction of about 20-40 wt.% of biomass [7]. It is composed of aromatic rings which are converted into high molecular char products during thermochemical processes. Hemicellulose is about a third of the mass of total dry biomass and is responsible for the cell wall, being a mix of polysaccharides, constituted by pentose and hexose monosaccharide units [8]. Some biomasses and their organic composition (Lignocellulosic structures) fraction by mass are shown below, in Table 2.

Table 2. Lignocellulosic composition.

Reference	Biomass	Cellulose	Hemicellulose	Lignin
[9]	Peanut straw	31.5	14.2	23.7
[9]	Soybean straw	37.8	18.8	19.7
[10]	Sawdust	18.0	12.6	33.9
[10]	Cornstalks	31.5	25.9	14.0
[7]	Pine wood	42.1	17.7	25.0
[7]	Almond shell	24.7	27.0	27.2

2.2 Biomass characterization

The first step for the investigation of the biomass potential as fuel is the characterization of its chemical constituents, which permits the determination of the quality and its specific properties, as well as the feasibility of the application according to possible environmental problems [4]. Two common analyses for biomass characterization are the Ultimate Analysis and the Proximate Analysis.

2.2.1 Ultimate analysis

The Ultimate Analysis (UA) can provide the biomass combustible fraction, through the assessment of the elemental composition: carbon (C), oxygen (O), nitrogen (N), hydrogen (H), and sulfur (S) [11], not accounting the amount of inorganic constituents (ASH), and water/moisture in an ASH and moisture-free basis. Sometimes, some elements may be avoided in the calculations, due to their low presence in the feedstock, such as sulfur [12]. The calculation of UA is given by Equation 1, below.

$$C + H + O + N + S = 100(wt)\% \quad (1)$$

2.2.2 Proximate analysis

More general than the ultimate analysis, the Proximate Analysis (PA) measures the gross content of Moisture (M), Fixed Carbon (FC), Volatile Matter (VM), and Ash (ASH) present in the biomass. This analysis indicates the biomass quality and allows the characterization of the produced biomass-based coal [11], and is a relatively inexpensive process [5]. Fixed Carbon (FC) is the solid carbon of biomass in char, which remains after devolatilization in the pyrolysis process. When fuel is heated, there are condensable and non-condensable vapors released Volatile matter (VM), depending on the rate of heating and the temperature employed in the process [5]. The calculation of PA is given by Equation 2, and the PA and UA for some biomasses are given in Table 3.

$$\mathrm{VM} + \mathrm{FC} + \mathrm{ASH} + \mathrm{Moisture} = 100(\mathrm{wt})\%$$

Table 3. Proximate and Ultimate analysis.

Reference	Biomass	Proximate Analysis					Ultimate Analysis					
		M	VM	FC	ASH	Total	C	H	O	N	S	Total
[13]	Palm leaves	5.0	78.1	5.2	11.7	100.0	49.4	5.8	42.3	1.2	1.3	100.0
[4]	Oak wood	6.5	73.0	20.0	0.5	100.0	50.6	6.1	42.9	0.3	0.1	100.0
[14]	Cellulose	4.7	93.4	1.9	0.1	100.1	41.7	5.7	52.2	0.4	0.0	100.0
[14]	Xylan	5.8	77.8	12.8	3.6	100.0	45.4	6.7	46.9	0.9	0.1	100.0
[14]	Lignin	3.4	60.4	32.6	3.6	100.0	61.3	5.1	31.7	1.1	0.7	100.0
[4]	Coal	5.5	30.8	43.9	19.8	100.0	78.2	5.2	13.6	1.3	1.7	100.0
[4]	Sewage sludge	6.4	45.0	5.3	43.3	100.0	50.9	7.3	33.4	6.1	2.3	100.0
[4]	Grape marc	10.0	59.2	23.8	7.0	100.0	54.0	6.1	37.4	2.4	0.2	100.1
[4]	Olive husks	6.8	73.7	17.4	6.8	104.7	50.0	6.2	42.1	1.6	0.1	100.0
[15]	White Pine	6.9	76.6	15.8	0.7	100.0	53.3	6.0	40.0	0.5	0.2	100.0

2.3 Thermochemical processes

Thermochemical processes are based on the use of heat to convert fuels such as biomass or coal, into other chemical products or even electrical energy. Some of them, are Pyrolysis, Combustion, Gasification, Torrefaction, and Liquefaction.

2.3.1 Drying

Water content in biomass affects directly carbon conversion, cold gas efficiency, and high heating value [16]. Normally, crude biomass possesses a percentage of moisture in its composition, in the range of 5-50% by mass. To reduce this content to compositions less than

10%, temperatures of 80 to 100°C are employed, at the beginning of the gasifier [17]. In this step, the biomass does not have any kind of chemical decomposition [18].

2.3.2 Pyrolysis

Pyrolysis is performed by heating biomass in the absence of pure air, or a medium partially supplied with oxygen and converting the biomass into liquid products, non-condensable gases, and charcoal [19]. In this process, with mainly endothermic reactions, huge hydrocarbon molecules from Cellulose, Hemicellulose, and Lignin are broken down into smaller products, with variable composition amounts, depending on the velocity and biomass composition at which it happens. For faster pyrolysis velocity, liquid fuels are dominant, whereas, for slower processes, higher gas and solid charcoal fractions are produced [5].

Tar is an important product of this process, resulting from the condensation of high molecular weight materials into liquids with viscous aspects, which generates problems in the process [12]. Some different Pyrolysis models and their descriptions are presented below in Table 4.

Table 4. Pyrolysis models.

Ref.	Pyrolysis models	Description
[20]	$C_{19.82}H_{24.52}O_{11.86} \rightarrow 5.96CO + 2.95CO_2 + 8.26H_2 + 1.5CH_4 + 0.5C_2H_4 + 8.41Char\ (\Delta H = 310.01\ kJ/mol)$	Biomass decomposition is represented by a generic formula and solved by a kinetic reaction
[21]	$Biomass\ component \rightarrow x1\ H_2 + x2\ CH_4 + x3\ CO_2 + x4\ H_2O + x5\ Carbon + x6\ C_6H_{6.2}O_{0.2}$	Biomass is represented by 5 main molecules (cellulose, hemicellulose, and 3 lignin), with five different reactions
[22]	$Biomass \rightarrow n_{CO}\ CO + n_{CO_2}CO_2 + n_{H_2}H_2 + n_{CH_4}CH_4 + n_{Char}Char + n_{Tar}Tar$	Biomass decomposition in a generic formula, and char with its own kinetic decomposition model
[23]	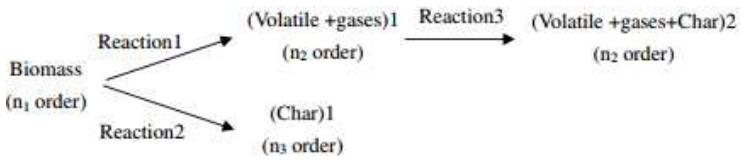	Three reactions, which Volatile + gases can react with char and cause other products (reaction 3)

Tar is an undesirable black and thick liquid product of pyrolysis and gasification zone, and is composed of a complex mixture of complex condensable hydrocarbons such as benzene,

toluene, and naphthalene, the majority. It can condense into cooler areas of the gasifier and cause its clogging; in the hotter areas, can polymerize into more complex structures, making the treatment hard [3]. The contamination of the Syngas with tar compromises its direct use in gas turbines or gas engines [24], as much as its use in many other commercial applications. So, it is suitable that the final gas possesses a value below 1g/Nm³ of tar, which can be lower depending on the final use [25]. Another reference [26] considered the maximum limit for tar amount in Syngas composition as 0.1g/Nm³.

2.3.3 Gasification

Gasification is partial combustion with a controlled flow rate of gasification agent (air, steam, or oxygen, which results in the conversion of hydrocarbons from biomass into carbon monoxide (CO), carbon dioxide (CO_2), hydrogen gas (H_2), water (H_2O), and methane gas (CH_4) [27] [12], being present too small amounts of char and condensable components [12]. The produced Syngas has been considered a promising process, due to the reduced amount of emissions, as well as a good way for treating the residual biomass [28].

2.3.4 Combustion

In combustion, the biomass is burned with oxygen at a rate of 4-5kg per kg of biomass [29] for a complete burn. When this process is used in the gasification of biomass, the oxygen injected by the oxidizing agent produces a mixture of carbon monoxide (CO), carbon dioxide (CO_2), and water (H_2O). Some amount of the tars is burned, producing heat, and the remaining is cracked into lower-weight hydrocarbons [13]. The reactions in this zone are mainly exothermic, and the system can reach temperature ranges of 1200-1450°C [30]. Therefore, the heat produced in this zone is reused in other parts of the system, due to the presence of endothermic reactions.

2.4 Gasifier

The gasifiers are divided into 3 main types, according to the mode of contact between gas and solid phases and the gasifying agent employed. In the fixed bed or moving bed, as it is also called, the fuel is supported by a grate, different from the two others (Entrained flow and Fluidized bed), in which the gasifying agent all converts the feedstock through the gasifier (see Figure 2).

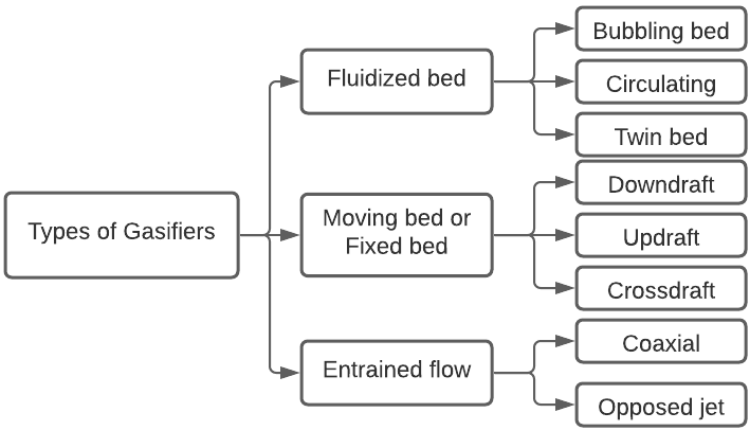

Figure 2. Divisions and subdivisions of gasifier types.

2.4.1 Updraft Gasifier

The fixed bed gasifiers are simple to project and usually have high carbon conversion, with long residence time and low gas velocity [31]. This is the simplest and oldest gasifier, having a relatively low cost to implementation [32]. The gasifying agent is fed by the bottom and flows up at the top, while, in countercurrent, the feedstock is fed at the top, flowing down under the gravity effect. The hottest temperature of this gasifier is near the bottom in the Combustion zone, where the gasifying agent reacts with the biomass, releasing heat by an exothermic reaction. Thereby, the tar produced near the top, in the Pyrolysis zone, meets the hot gas at a low temperature, not having an opportunity for new cracking [5]. Figure 3 shows an Updraft gasifier scheme, with the different zones, inputs, outputs, and the representation of the hottest area.

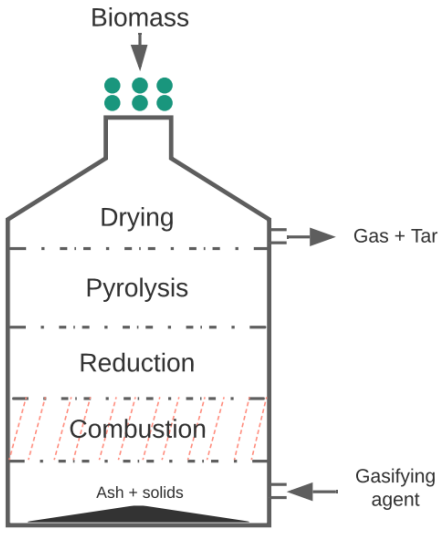

Figure 3. Updraft gasifier and its shift zones.

2.4.2 Downdraft Gasifier

In this gasifier, the fuel and gasifying agent are fed on the top, flowing concurrently to the bottom. Due to most of the biomasses having great amounts of volatile matter in their composition, keeping it up in contact with the gasifying agent during the flowing down, causes conversions until 99,9% of the tar [33]. In the Combustion zone (oxidation zone), the temperature should be maintained as high as possible, near 1000ºC [31], providing heat to the adjacent zones (Pyrolysis and Reduction), improving energy efficiency. Chanthakett et al., 2021 [34] state that the produced Syngas in a Downdraft gasifier shows compositions around 13-18% of CO and 11-16% of H_2 by volume. Below, a scheme for a Downdraft gasifier is presented in Figure 4.

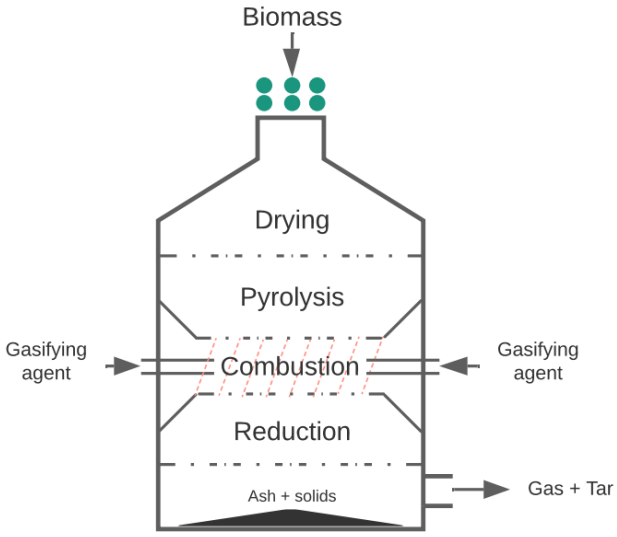

Figure 4. Downdraft gasifier and its zones.

2.5 Reactions

In a Syngas production process, there are many reactions involved, being almost impossible to predict and input into a model all the possible ones. Thereby, it can be selected a set of main reactions, building a model that approaches reality and provides reliable results. Below, in Table 5, there are shown the selected reactions considered to create this model.

Table 5. Some possible reactions in a Syngas production process.

Stage	ID	Reaction	Description	ΔH (kJ/mol)	Reference
Pyrolysis	R(1)	$Biomass \rightarrow Char + Gas + Tar$	Pyrolysis reaction	-	
Combustion	R(2)	$CO + \frac{1}{2}O_2 \rightarrow CO_2$	Carbon Monoxide Oxidation	-282.9	[5]
	R(3)	$C_{(s)} + \frac{1}{2}O_2 \rightarrow CO$	Carbon Partial Oxidation	-110.6	[5]
	R(4)	$C_{(s)} + O_2 \rightarrow CO_2$	Carbon Oxidation	-393.5	[5]
	R(5)	$CH_4 + 2O_2 \rightarrow CO_2 + 2H_2O$	Methane Oxidation	-801.7	[5]
	R(6)	$H_2 + \frac{1}{2}O_2 \rightarrow H_2O$	Hydrogen Oxidation	-241.5	[5]
	R(7)	$C_{10}H_8 + 12O_2 \rightarrow 10CO_2 + 4H_2O$	Naphthalene Oxidation	-5157.0	[35]
	R(8)	$C_7H_8 + 9O_2 \rightarrow 7CO_2 + 4H_2O$	Toluene Oxidation	-3910.0	[35]
	R(9)	$C_6H_6 + 7{,}5O_2 \rightarrow 6CO_2 + 3H_2O$	Benzene Oxidation	-3268.0	[35]
Heterogeneous Reduction	R(10)	$C_{(s)} + CO_2 \rightarrow 2CO$	Boudouard Reaction	172.0	[5]
	R(11)	$C_{(s)} + H_2O \rightarrow CO + H_2$	Carbon Reforming	131.0	[5]
	R(12)	$C_{(s)} + 2H_2 \rightarrow CH_4$	Hydrogasification	-74.8	[5]
Homogeneous Reduction	R(13)	$CH_4 + H_2O \rightarrow CO + 3H_2$	Steam-methane Reforming	206.0	[5]
	R(14)	$CO + H_2O \rightarrow CO_2 + H_2$	Water Gas Shift Reaction	-41.2	[5]

2.6 Parameters

2.6.1 Heating values

This property is divided into two types: Higher Heating Value (HHV) and Lower Heating Value (LHV). The former means the amount of heat that is released by a certain quantity of mass of fuel required for the process, still counting the latent heat of vaporization of water contained (moisture) in the fuel. The latter (LHV) is defined as the amount of heat released by the combustion of a fuel, deducting the latent heat of vaporization of water contained in the combustion gas product [5]. Both values have a dimension of MJ/Nm^3, which correspond to the heat released (MJ) per normal cubic meter (Nm^3), the volume occupied by the gas in standard conditions.

2.6.2 Oxidation and reduction mediums

There are four mediums: air, steam, carbon dioxide, and steam-oxygen. It is an important parameter to be analyzed because of its influence on tar production. From the rate of medium inserted in the process, it is possible to calculate the parameter that relates it to the rate of biomass. The parameters vary according to the medium to which are referred. When air (or pure oxygen gas) is employed as an oxidant medium, the parameter calculated is called

Equivalence ratio (ER), for steam, is the Steam-to-biomass ratio (S/B), for oxygen Steam-oxygen, is Gasifying ratio, and CO_2-to-biomass ratio [5]. Steam is feasible to produce high-H_2-Syngas, increasing this content as S/B increases from 0.25 to 1.0.

2.6.3 Temperature

It is very important to maintain the temperature closer to the optimum to rise the components conversion. According to Le Chatelier's principle, temperature increase favors the products of the endothermic reactions, while, for exothermic reactions, it favors the reactants. Pyrolysis has mainly endothermic reactions, Combustion reactions are mainly exothermic, and Gasification is globally endothermic. Ahmad et al., 2016 [32], conclude that higher temperatures contribute to tar cracking in lower-weight products and much lower concentrations of char. Still, the gas yields are greater due to the release of more volatiles. So, higher temperatures in gasification generate fewer solids and tar emissions, decreasing the post-treatment needs of the produced gas to purify it [18].

2.6.4 Pressure

Depending on the application of the Syngas, the pressure in the gasifier can vary between the atmospheric (1 bar) and elevated pressures (up to 33 bar) [32]. According to Asadullah, 2014 [31], higher pressures contribute to decreasing tar yield in the product gas.

2.6.5 Atomic ratios

Oxygen-to-carbon ratio (O/C) is the atomic ratio between the two elements available in the fuel. It correlates with the fall in the Higher Heating Value while the O/C ratio increases. When the Hydrogen-to-carbon ratio (H/C) increases, the Effective Heating Value (or Lower Heating Value (LHV) as is named) of the fuel decreases [5]. Oxygen, carbon, and hydrogen mass fractions and H/C and O/C ratios for some selected biomasses are shown in Table 6.

Table 6. O/C and H/C atomic ratio.

Reference	Biomass	C	H	O	H/C	O/C
[13]	Palm leaves	49.40	5.80	42.30	1.40	0.64
[4]	Oak wood	50.60	6.10	42.90	1.44	0.64
[4]	Coconut shells	51.10	5.60	43.10	1.31	0.63
[4]	Soya husks	45.40	6.70	46.90	1.76	0.78
[4]	Chicken litter	60.50	6.80	25.30	1.34	0.31
[4]	Coal	78.20	5.20	13.60	0.79	0.13
[4]	Sewage sludge	50.90	7.30	33.40	1.71	0.49
[4]	Grape marc	54.00	6.10	37.40	1.35	0.52
[4]	Olive husks	50.00	6.20	42.10	1.48	0.63

2.6.6 Biomass composition

According to Qin et al., 2015 [10], the raw biomass chemical properties provide important information about the products. Cellulose has a higher O/C ratio and volatile matter than lignin, generating more CO and less H_2 [36]. In their study, Tian et al., 2017 [16], reported that cellulose and hemicellulose produce gases more quickly, and are rich in CH_4 and CO, than lignin, which produces gases with higher amounts of H_2 and CO_2, and is more suitable to H_2-rich-gases.

2.6.7 Syngas expected

The quality of the Syngas produced depends on some indices such as carbon conversion, H_2/CO ratio, CH_4/H_2 ratio, Gas yield, and Gasification efficiency [37]. Another way, the standard high-quality, to evaluate the quality of the Syngas produced is a high amount of H_2 with lower tar components in the Syngas composition [38]. Second [26], the composition of Syngas for fixed-bed gasifiers is 8 to 9% for CH_4, 26 to 27% for CO_2 and CO, and 36 to 39% for H_2, considering Syngas free of N_2.

2.7 Software

Simulating systems is a good way to understand how the process behaves when a part of it is changed, thus allowing to evaluate actions and strategies in order to develop and improve the dynamics of the system, obtaining a certain level of accuracy in relation to reality. First, it is necessary to represent the process, using mathematical models based on experimental data, and conducting virtual experiments which are tested, changed, and enhanced. For a chemical process, models are constructed according to mass, energy, and momentum balances. Researches using different softwares as well as the aim, gasifying agent, gasifier, and biomass employed in each, are shown in Table 7.

Table 7. Gasification simulation works using different software.

Reference	Biomass	Software	Gasifier	Aim	Gasifying agent
[39]	White pine	Aspen Plus	-	Predicting the gas yield, LHV, CCE, CGE	Steam
[40]	Palm kernel shell	Aspen Plus	Fluidized bed	Optimizing conditions to maximum H_2 and Syngas composition	Steam
[41]	Rice husk	Ansys Fluent	Updraft	Comparison between the resulted Syngas using two gasifying agents	Air and Air-steam
[13]	Date palm leaves	Aspen HYSYS	Downdraft	Predicting the gas composition and finding optimal operations conditions	Steam
[42]	Hardwood	UniSim Design	-	Decrease tar formation by a combination between low and high stages gasification temperatures	Steam
[43]	Pinus radiata	UniSim Design	Dual Fluidized bed	Discover the effect of gasification temperature; (S/B); air supplied; moisture biomass content, in energy and exergy efficiencies	Steam
[44]	Rice straw	COCO	-	Achieve the optimum values of variables according to their interaction	Air

2.7.1 UniSim Design

UniSim Design Suite, by Honeywell, is a suitable process design software able to create systems in steady-state or dynamic simulations, as much yield estimation, financial planning, process optimization, and cost administration [45]. The software has a database of components to be utilized in the design and is possible to generate new solid hypothetical components through their Ultimate and Proximate analysis. It still permits the creation of the flow sheeting of the process, adding, when necessary, equipment and reaching automatically mass and heat balances.

The Gibbs reactor acts to reach reaction equilibrium by maximizing entropy when provided the pressure and heat duty or minimizing the Gibbs free energy, which happens when the temperature and pressure are specified by the simulation [46]. In the simulation, still is

possible to choose inert compounds, as well as define fractions expected about some components present. Specific Equilibrium reactions can be added, for known reactions stoichiometry, or let the software reach the equilibrium through Gibbs reactions.

The reactor Yield Shift reactor unit is based on data tables to perform shift calculation and is used when the reactions are complexes, and the models are not available, or too computationally expensive [47]. The shift can be done using two pieces of information, depending on what is known by the user: Yield only or Yield with Percent conversion. Still, will be needed to supply some basis for calculation, as much as the mass flow, or mole flow, and the most important is that the sum in the shift step needs to be equal to 0, ie, the mass balance for the reactants is equal for the products.

2.8 Model

To calculate the yield and products of the process in a gasifier, there are three methods that can be used: the Kinetic model (KM), the Computational Fluid Dynamic model (CFD), and the Equilibrium model (EM) [48].

2.8.1 Kinetic Model

In a Kinetic Model is necessary the knowledge of the kinetic parameters for all reactions present in the gasifier for the calculation of the reaction rates, together with the reactor hydrodynamics and the residence time. It predicts how fast the products of the reactions are formed [5] and the profile of the product gas composition, according to operating conditions and configuration of the gasifier, as well as its performance [3]. In contrast, Kinetic Models can be very difficult to implement due to the need for experimental parameters.

2.8.2 Equilibrium Model

The Thermodynamic Equilibrium models predict a way to reach the maximum yield of a product in a determined reacting system, that is the extent of reaction progress [5]. It does not consider the geometry and other characteristics of the design, being a model-independent of the gasifier and unsuitable for studying the influence of parameters like fluidizing velocity, radium or height of gasifier, hydrodynamic performance, etc [3]. This model is divided into two categories: the Stoichiometric model, which needs equilibrium constants of any reaction involved in the process, and the second one, the non-Stoichiometric model, which is carried out by minimizing the Gibbs free energy [48]. Below, in Table 8, some references are presented with the models, gasifier types, and feedstocks employed.

Table 8. Model-based works and other parameters (Feedstock and Gasifier).

Reference	Model	Feedstock	Gasifier
[48]	EM	$CH_aO_bN_cS_d$	Downdraft
[49]	EM	Hazelnut shell	Fluidized bed
[50]	CFD	Woody biomass	Entrained flow
[17]	EM	Rice husk; Larch wood and Wood chips	-
[41]	CFD	Rice husk	Updraft
[51]	KM	Pine; Maple-oak mixture; Seed corn; Corn stover; Switch-grass	Fluidized bed
[52]	CFD	Wood chips	Downdraft
[53]	KM	Wood	Fluidized bed

3 METHODOLOGY

Three different agricultural biomasses were chosen: Olive residue; corn straw, and grape marc. Below, in Table 9, the UA and PA for each biomass are shown.

Table 9. Ultimate and Proximate analysis of chosen biomasses for the simulation.

Reference	Biomass	Proximate Analysis					Ultimate Analysis					
		M	VM	FC	ASH	Total	C	H	O	N	S	Total
[4]	Grape marc	10.0	59.2	23.8	7.0	100.0	54.0	6.1	37.4	2.4	0.15	100.05
[4]	Corn straw	7.4	67.7	17.8	7.1	100.0	48.7	6.4	44.1	0.7	0.08	99.98
[4]	Olive residue	10.6	60.2	22.8	6.4	100.0	58.4	5.8	34.2	1.4	0.23	100.03

The Syngas production process was considered into 4 main steps: the Drying of moisture present in the biomass until 5% w/w, followed by Pyrolysis, which was split into Devolatilization, and Char cracking, both calculated with the help of Microsoft Excel. In Combustion, were added oxidation equilibrium reactions, and the Reduction process was divided into heterogeneous, and homogeneous steps, being inserted into the equilibrium reactions in UniSim Design. The process steps can be seen in Figure 5.

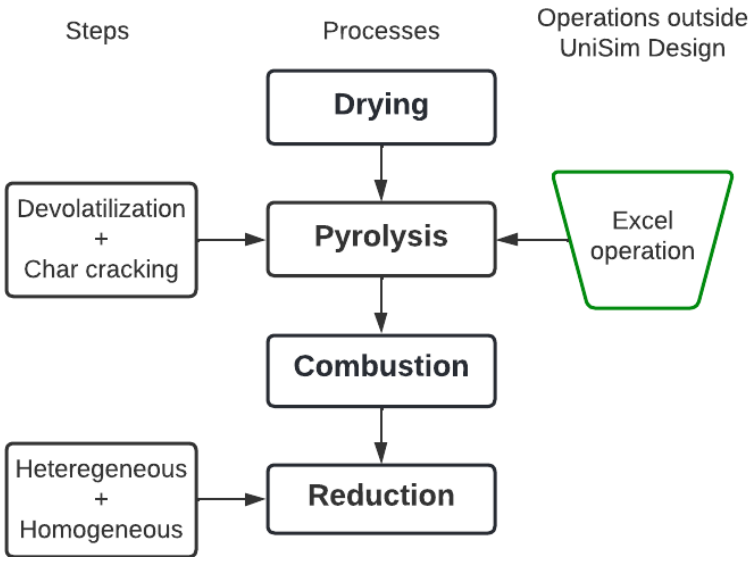

Figure 5. Division of the Syngas synthesis process.

3.1 Considerations

The construction of the model implied the application of some considerations listed below:

- Operation of the process occurs in Steady-State;
- Peng-Robinson was selected as the thermodynamic Fluid Package (FP) for the simulation;
- Tar is constituted of three main components: benzene (60%), toluene (20%), and naphthalene (20%), by mass;
- Char is broken into its main constituents ($C_{(s)}$, O, H, N, $S_{(s)}$, H_2O);
- ASH is removed in the middle of the process;
- Air is 79% of nitrogen (N_2) and 21% of oxygen (O_2), on a molar basis;
- Nitrogen (N_2) and sulfur ($S_{(s)}$) are considered inert during the processes;
- Reduction is split into Heterogenous and Homogeneous Reactions;
- All process is operated under atmospheric pressure, and pressure drops are disregarded;
- Solid carbon is mainly consumed in the Reduction zone;
- It is considered the standard high-quality Syngas;
- The process is partially adiabatic.

3.1 Setup

The first view of UniSim Design, Simulation Basis Manager (SBM), is an area to input the components which will be present on flow streams, as well as, the Fluid Package, which determines the thermodynamic method used to calculate variations during the process, most of the times, vapor-liquid equilibria; there is the input of reactions, which can be defined by the type, as Equilibrium, Kinetic, Conversion, Simple rate.

The software has some solids in its library to add to the system, such as carbon and sulfur, however, when it concerns biomass residues, it does not have the standard composition for each type of biomass. Thus, there is another area in the Simulation Basis Manager called Hypotheticals, where it is possible to add and simulate hypothetical biomasses, being necessary to know only the properties of Proximate and Ultimate analysis, and after the input, the software calculates other information as Molecular weight and Density for this compound. Therefore, it is possible to create, not only biomasses and coal solids, but even ASH, putting the compound as 100% by mass of this component. This place possibilities to insert all reactions necessary to the process and link them with the corresponding Fluid Package chosen.

3.2 Downdraft Simulation view

The simulation of biomass gasification for all biomasses in a Downdraft type gasifier can be seen in Figure 6 below.

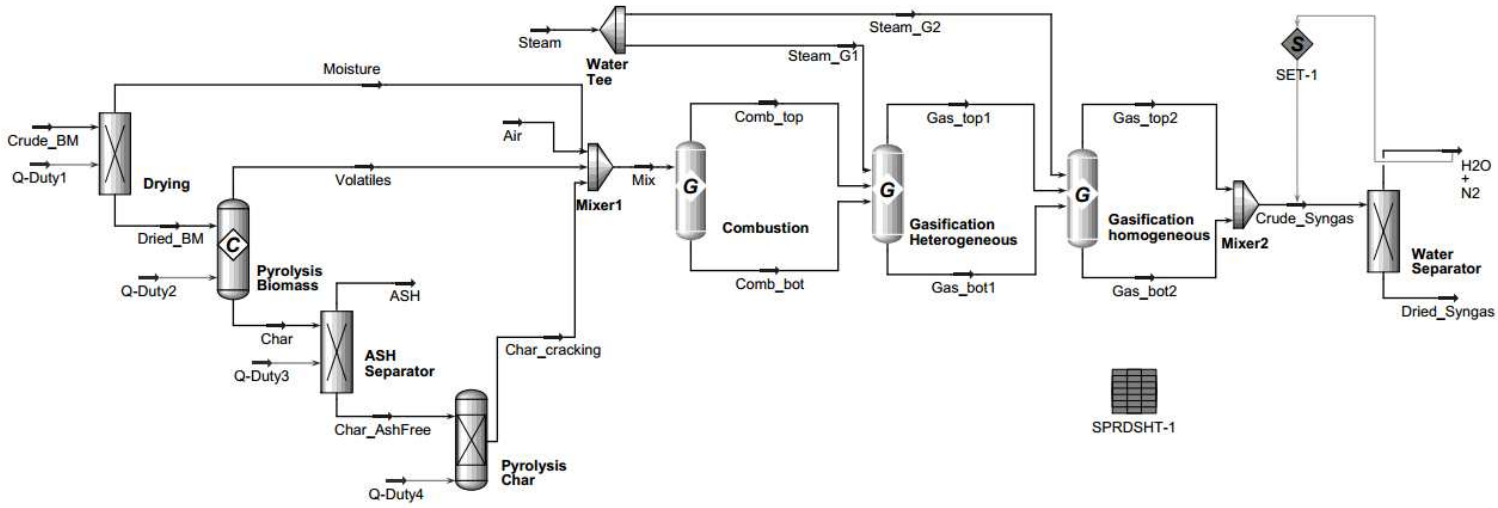

Figure 6. General View of the Biomass gasification simulation in a Downdraft gasifier.

3.2.1 Downdraft Modeling

Figure 6 presents the simulation for all biomasses, and Table 5 presents the reactions that participate in the process. The methodology will be accompanied by the simulation steps.

The calculation basis used for all biomasses entering the system was a flow of 10kg/h, after the Drying step.

3.2.1.1 Drying Model

The drying phase was based on the total amount of moisture (M) present in biomass in order to achieve 5% by mass of moisture in the line.

3.2.1.1.1 Drying simulation

Crude biomass named “Crude_BM” enters on a Splitter named “Drying”, which operates at 150°C, supplied by “Q-Duty1” energy line, to remove the moisture excess, named “Moisture”. Then, the dried biomass, named “Dried_BM”, has its PA recalculated, considering the set value of moisture at 5%. This new biomass is inputted as a hypothetical solid and

followed to the first step of Pyrolysis in the reactor named "Pyrolysis Biomass". The new values for each dried biomasses can be seen in Table 10, below.

Table 10. Modified values in PA for Dried biomasses.

Dried Biomasses	Proximate Analysis				
	M	**VM**	**FC**	**ASH**	**Total**
Grape marc	5.0	62.5	25.1	7.4	100.0
Corn straw	5.0	69.5	18.3	7.3	100.0
Olive residue	5.0	64.0	24.2	6.8	100.0

3.2.1.2 Pyrolysis Model

Pyrolysis products were considered as three main groups: Gases (CO_2, CO, H_2, CH_4), tar (C_6H_6, C_7H_8, $C_{10}H_8$), as benzene, toluene, and naphthalene, respectively, and Char plus ASH in the solid line, as Figure 7 shows.

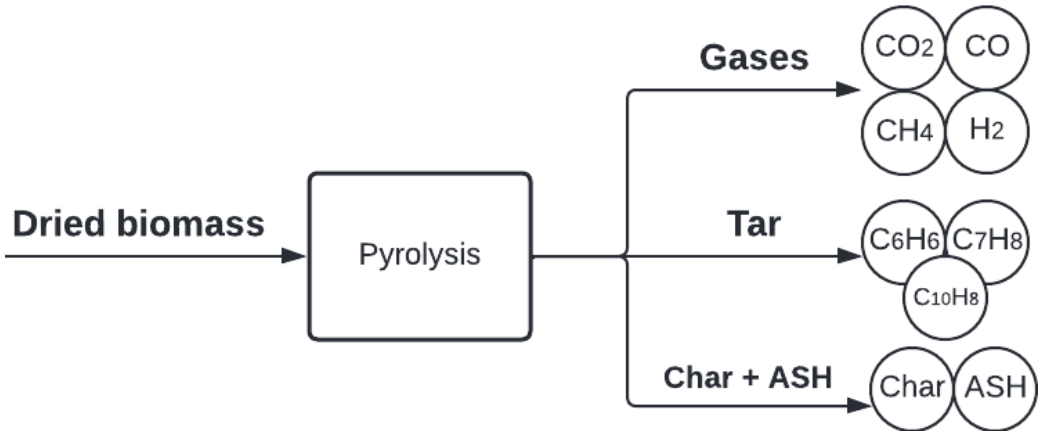

Figure 7. Pyrolysis products.

In order to estimate the yields and stoichiometric coefficients of the reactions in the Pyrolysis process it was followed a methodology [54] based on second-order equations with Pyrolysis process temperature as the variable, to calculate the mass fraction of each main component (Char, Tar, and Gas) by mass (w/w), and the second block of components inside Tar and Gas composition. The calculations were possible with the help of an Excel spreadsheet, using the equations shown below.

$$Y_{Char} = 7.97 \times T^2 \times 10^{-5} - 0.125 \times T + 68.87$$

$$Y_{Tar} = -1.38 \times T^2 \times 10^{-4} + 0.12 \times T + 12.64$$

$$Y_{Gas} = 1.12 \times T^2 \times 10^{-4} - 0.058 \times T + 30.77$$

Inside the Gas fraction, the mass fraction of the main gases produced by Pyrolysis is followed by the equations below.

$$Y_{CO} = -2.65 \times T^2 \times 10^{-4} + 0.27 \times T - 32.71$$

$$Y_{CO_2} = -2.85 \times T^2 \times 10^{-5} - 0.029 \times T + 70.89$$

$$Y_{CH_4} = 6.69 \times T^2 \times 10^{-5} - 0.037 \times T + 4.28$$

$$Y_{H_2} = 7 \times T^2 \times 10^{-5} - 0.0371 \times T + 5.1117$$

Inside the Tar fraction, were considered fractions of 60%, 20%, and 20% of benzene, toluene, and naphthalene [32], respectively, as shown below.

$$Y_{C_6H_6} = 0.6 \times Y_{Tar}$$

$$Y_{C_7H_8} = 0.2 \times Y_{Tar}$$

$$Y_{C_{10}H_8} = 0.2 \times Y_{Tar}$$

Another reaction present in this step is the conversion of the ASH present in the biomass.

$$(-1)\text{DriedBiomass} \rightarrow \left(\frac{MM_{db}}{MM_{dbfASH}}\right) \times \left(\frac{m_{dbfASH}}{m_{db}}\right) \times \text{DriedBiomass}_{freeASH} + \left(\frac{MM_{db}}{MM_{ASH}}\right) \times \left(\frac{m_{ASH}}{m_b}\right) \times \text{ASH}$$

Reaction 1

Where:

- MM_{dbfASH}: Molar mass of dried and ASH-free biomass;
- MM_{ASH}: Molar mass of ASH;
- m_{ASH}: Mass of ASH.

Therefore, new biomasses were created considering ASH as 0 in the PA, normalizing the other values and UA continuing as before. The new values for PA for each biomass are shown in Table 11, below.

Table 11. Modified values in PA for Dried Ash-Free Biomasses.

Dried Ash-Free Biomasses	**Proximate Analysis**				
	M	**VM**	**FC**	**ASH**	**Total**
Grape marc	5.41	67.46	27.12	0.00	100.00
Corn straw	5.40	74.91	19.69	0.00	100.00
Olive residue	5.38	68.63	25.99	0.00	100.00

For the reactions of the components inside the gas fraction, it was necessary to calculate the fractional conversion of each product of Pyrolysis. For that, it was employed the equation shown below.

$$FC_{Gas,i} = \frac{(\dot{m}_{bfASH} \times Y_{G,i})}{\dot{m}_b} \times \left(\frac{Y_{Gas}}{100}\right)$$

Where:

- $FC_{Gas,i}$: Fractional conversion of each component *i* inside the gas mass fraction;
- $Y_{G,i}$: Mass fraction of each component in the gas produced;
- $\dot{m}_{bfASH}$: Mass flow of biomass-free ASH;
- $\dot{m}_b$: Mass flow of biomass.

The fractional conversion inside the products of Tar was considered equal for each component because the mass fraction and the equation used to calculate is equal to the gases fraction conversion.

$$FC_{Tar,i} = \frac{(\dot{m}_{bfASH} \times Y_{T,i})}{\dot{m}_b} \times \left(\frac{Y_{Tar}}{100}\right)$$

Where:

- $FC_{Tar,i}$: Fractional conversion of each component *i* inside the Tar mass fraction;
- $Y_{T,i}$: Mass fraction of each component in Tar produced;
- $\dot{m}_{bfASH}$: Mass flow of biomass-free ASH;
- $\dot{m}_b$: Mass flow of biomass.

3.2.1.2.1 Pyrolysis Simulation – Step 1

After the calculations in the Excel spreadsheet, it was possible to add the Conversion reactions of each component on SBM, and link them to the FP.

All reactions were employed in a Conversion Reactor called “Pyrolysis Biomass”, supplied by an energy stream “Q-Duty2”. Gases and Tar components formed in this step of Pyrolysis are sent in the current “Volatiles” to a mixer “Mixer1” to mix with the other currents.

3.2.1.2.2 Pyrolysis Simulation – Step 2

Char and ASH are sent through the line “Char” to a Splitter “ASH Separator”, removing the ASH from the process. The current “Char_AshFree” goes to the second step of Pyrolysis in a Yield reactor “Pyrolysis Char” to transform the Char into its elemental components: Solid

carbon ($C_{(S)}$), oxygen gas (O_2), hydrogen gas (H_2), nitrogen gas (N_2), solid sulfur ($S_{(S)}$), and water (H_2O), resulted from the moisture, as shown in the equation below.

$$\text{Char} = C_{(s)} + O_2 + H_2 + N_2 + S_{(s)} + H_2O$$

Therefore, the amount of solid carbon, nitrogen gas, and solid sulfur is achieved by the UA. Although, to reach the amount of hydrogen gas and oxygen gas, was considered how much water there was in biomass composition, to know how many moles of oxygen and hydrogen belong in moisture content. This value was subtracted for each element (H_2, O_2), and the result was employed in the reactor as base yields.

This data, resulting from the Char cracking of each biomass, is shown below in Table 12.

Table 12. Mass and Mole results of Char cracking for each biomass on the second Pyrolysis stage.

	Olive residue		**Corn straw**		**Grape marc**	
Composition (%)	**Mass**	**Mole**	**Mass**	**Mole**	**Mass**	**Mole**
$C_{(s)}$	58.38	55.78	48.71	47.78	53.97	52.09
O_2	29.41	10.55	39.30	14.47	32.57	11.80
H_2	5.20	29.59	5.80	33.89	5.49	31.57
H_2O	5.38	3.43	5.40	3.53	5.41	3.48
N_2	1.40	0.57	0.70	0.29	2.40	0.99
$S_{(s)}$	0.23	0.08	0.08	0.03	0.15	0.05

3.2.1.3 Combustion Model

The combustion step was considered adiabatic to verify the temperature dynamic according to the airflow inputted. Each compound had the Combustion Equilibrium Reaction added on SBM, and the ER was calculated considering the stoichiometric and actual rates.

3.2.1.3.1 Combustion Simulation

The line "Char_cracking" joins to the line "Volatiles" and "Air" in the equipment "Mixer1" to proceed to the Combustion zone, through the line "Mix" until "Combustion" equipment.

In this zone it was employed a Gibbs reactor, specifying the equilibrium reactions, being present the reactions "R2" Carbon Monoxide Oxidation, "R3" Carbon Partial Oxidation, "R4" Carbon Oxidation, "R5" Methane Oxidation, "R6" Hydrogen Oxidation, "R7" Naphthalene Oxidation, "R8" Toluene Oxidation, "R9" Benzene Oxidation, as Table 5 shows. It is supplied

Oxygen to the Combustion by the line “Air”, and the products “Comb_top” and “Comb_bot” follow to the first step of the Reduction zone.

3.2.1.4 Reduction Model

The reduction was split into Heterogeneous and Homogeneous, where the first one corresponds to the Gas-solid reactions and the second one to the Gas-Gas reactions. It is necessary to supply the process with a current of Steam, following the S/B ratio, due to the Reduction of Equilibrium Reactions added on SBM.

3.2.1.4.1 Reduction Simulation – Step 1

A line of steam called “Steam” is divided into two lines “Steam_G1” and “Steam_G2”. Products from Combustion and one of these lines of Steam “Steam_G1” supply the Gibbs Reactor “Gasification Heterogeneous” where the residual solid carbon is converted into gaseous products, following the reactions “R10” Boudouard Reaction, “R11” Carbon Reforming and “R12” Hydrogasification. The products from this equipment “Gas_top1” and “Gas_bot1” follow to the second and last step of the Reduction zone.

3.2.1.4.2 Reduction Simulation – Step 2

The last Gibbs Reactor “Gasification Homogeneous” is employed for the gaseous equilibrium reactions “R13” Steam-methane Reforming and “R14” Water Gas Shift Reaction, and the products, “Gas_top2” and “Gas_bot2” join in a Mixer “Mixer2”, resulting in a current “Crude_Syngas”, which goes to a Splitter “Water Separator” to separate the Water, resulting in the lines “H2O+N2” and the dried Syngas called “Dried_Syngas”.

4 RESULTS AND DISCUSSION

The first results are focused on the Pyrolysis process to analyze how the simulation behaves under different Pyrolysis temperatures.

4.1 Pyrolysis focus

First, the components resultant from Pyrolysis were plotted, varying the temperature of the process, considering the interval of 300 to 600°C. The variation of each component (Char, Tar, and Gas) can be seen in Figure 8, below.

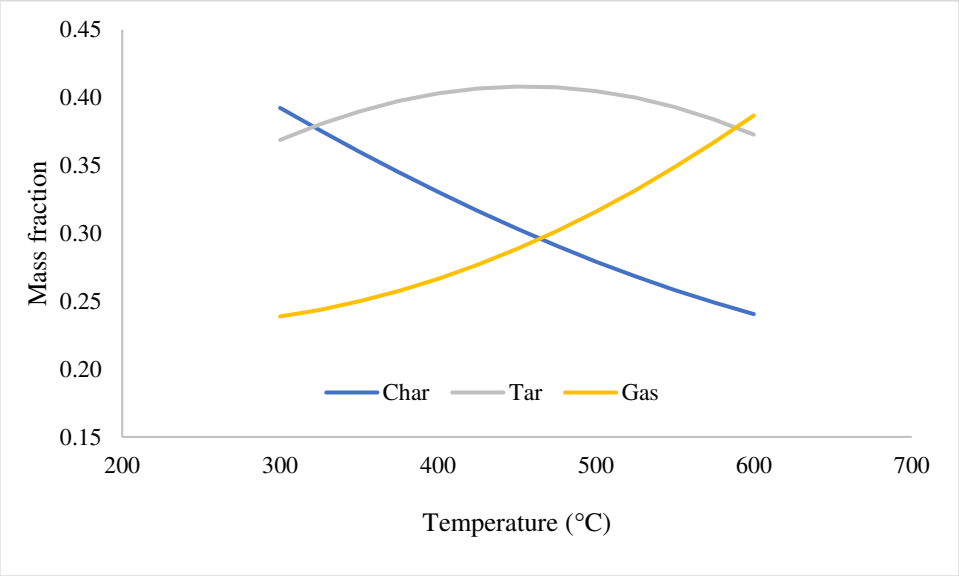

Figure 8. Variation of components mass fraction yields according to Pyrolysis temperature variation.

The curves of Figure 9 show a decrease in Char mass fraction as the temperature rises. The opposite is seen for the Gas mass fraction, which decreases with the increase in temperature of the Pyrolysis process. Tar mass fraction has a different behavior, once there is an area, between 400 and 500°C, that shows the highest mass fraction conversion, while decreases for lower and higher temperatures out of this interval. The same behavior for Char and Tar components was noted by Demirbas, 2007 [55], in addition to being reported that the tar highest yields are in the interval of 377 to 527°C, agreeing with the concavity top of Tar given by the model employed. In turn, Hanif et al., 2016 [56] reported on their work on the effects of Pyrolysis temperature on Product Yields, using Cotton Gin trash, Cow manure, and Microalgae as biomasses sources, that beyond 500°C, tar yield decreases, releasing the volatiles, and favoring the increase of gaseous products.

After that, the resultant Syngas variation with the Pyrolysis temperature was analyzed, to know how this parameter affects the products.

Then, the ER and S/B ratios are constant, and the temperature of the Pyrolysis was tested at 400, 500, and 600°C for olive residue biomass. This step was done in the Downdraft gasifier to understand how the behavior of the produced Syngas and if it is coherent with the literature. The second-order equations for the Pyrolysis process were applied for these temperatures, and the mass fractions are shown below in Table 13.

Table 13. Mass fraction for each component.

Component mass fraction	**400°C**	**500°C**	**600°C**
Y_{Char}	0.3305	0.2791	0.2405
Y_{Tar}	0.4030	0.4049	0.3727
Y_{Gas}	0.2664	0.3160	0.3868
Y_{CO}	0.3684	0.3923	0.3710
Y_{CO_2}	0.6130	0.5362	0.4733
Y_{CH_4}	0.0021	0.0273	0.0675
Y_{H_2}	0.0165	0.0442	0.0882

Below, in Table 14, are the results of the conversion reactions implemented in the "Pyrolysis Biomass" plus the results of the Yield Reactor "Pyrolysis Char" for different temperatures of Pyrolysis.

Table 14. Mass and mole composition of main components of Line "Mix" for olive residue for different temperatures in the Pyrolysis zone.

Component (%)	**400°C**		**500°C**		**600°C**	
	Mole	Mass	Mole	Mass	Mole	Mass
CH_4	0.08	0.06	1.15	0.83	3.03	2.59
C_6H_7	2.09	8.14	1.87	7.79	1.50	7.39
C_6H_6	7.38	24.43	6.63	23.38	5.32	22.17
$C_{10}H_8$	1.50	8.14	1.35	7.79	1.08	7.39
O_2	7.02	9.52	5.48	7.91	4.26	7.26
$C_{(s)}$	37.13	18.90	29.00	15.71	22.50	14.41
CO	8.35	9.92	9.44	11.93	9.53	14.23
CO_2	8.85	16.50	8.21	16.31	7.74	18.16
H_2	24.89	2.12	30.17	2.74	43.39	4.67

The main components present in the line "Mix" are shown in Figure 9, where it is plotted the mole composition variation versus the Pyrolysis temperature variation.

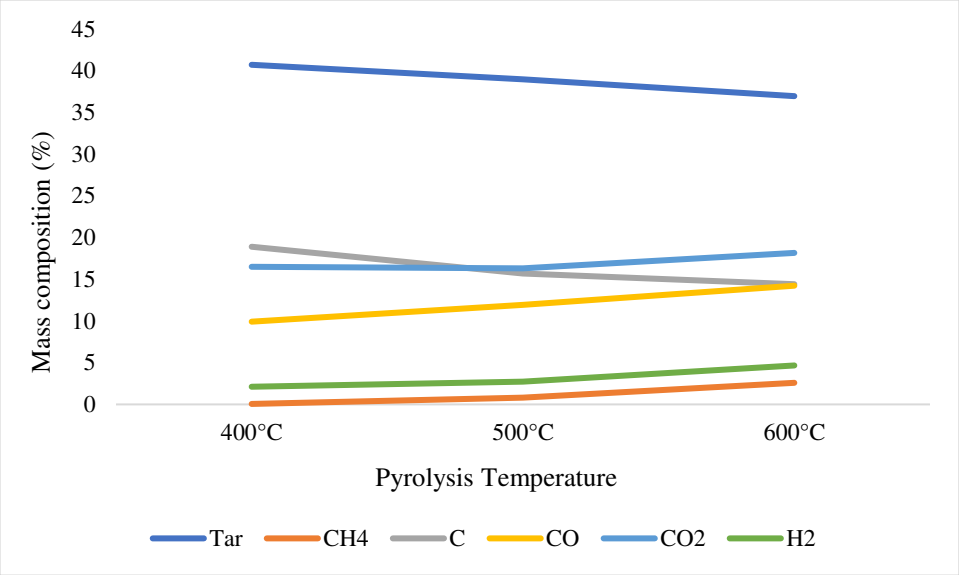

Figure 9. Component mass variation of line "Mix" according to Pyrolysis temperature variation.

It is possible to note the linear decrease of carbon with the increase in temperature, reducing almost 24% by mass (18.90–14.41), in the temperature interval of 400 to 600°C. The total tar presents the same behavior, however with a slight decrease. All gases, carbon monoxide (CO), methane (CH_4), hydrogen (H_2), and carbon dioxide (CO_2) present a tendency to increase according to the increase in temperature, emphasizing the abrupt rising in hydrogen, which more than doubled by mass, and the methane, in the same temperature interval. Ismail et al., 2020 [57] reported in their work about coal and biomass Pyrolysis in a fluidized-bed reactor, an increase in the total gaseous Pyrolysis yields, with exception of CO_2, in the interval of 500 to 600°C. Another work by Glushkov et al., 2021 [58] shows that CO_2, H_2, and CH_4 amounts increase as the Pyrolysis temperature increases (300-700°C), while the CO amount increases until 500°C, and after this temperature, starts to fall. Another similar study, using Anaerobic Sludge as biomass to verify the influence of Pyrolysis temperature in the product distribution, conducted by Hanif et al., 2019 [59], shows the same tendency for most Pyrolysis products by volume when the temperature is varied from 400 to 600°C. Hydrogen, and methane increase with temperature increasing, while CO_2 decreases, and CO firstly increases until 500°C, and after decreases until 600°C. The HHV accompanies H_2 and CH_4 rising, once the value more than tripled, in the same temperature variation (400-600°C), as a consequence of a great share of methane in the gas Heating Value.

4.2 Temperature effect in the Syngas characteristics

In general, the gasification reactions are mainly endothermic, and the process is very susceptible to variations in temperature, due to the equilibrium shift of the existent reactions in the process. At low temperatures, the CH_4 content is maintained, but above 600°C, is consumed due to the Methane reforming [28]. In turn, H_2 content is favored by this CH_4 consumption, increasing also with temperature rises. In this way, the LHV and HHV tend to decrease, once CH_4 supplies the biggest parcel. The trend of CO and CO_2 are not well comprehended, once there is a difference in results for distinct works. For instance, Hu et al., 2016 [60] with catalytic Syngas production of Sewage sludge, reached the raise of CO content and falling of CO_2 with temperature increase. The same behavior is shown by Nipattummakul et al., 2010 [61], moreover the reduction in the tar amount, as well as the consumption of CH_4 and the initial ascent in H_2 content followed by its descent. On the other hand, using Municipal solid waste supported by a catalyst of NiO, Wang et al., 2012 [62], reached an increment in volume fraction of CO_2 and H_2, while CO, CH_4, and tar decreased. Luo et al., 2009 [63], also had similar results in a study about temperature and steam influence.

In a study using NiO supported by dolomite as a catalyst to produce Hydrogen-rich Syngas, Wang et al., 2012 [62] tested different reactor temperatures, from 700 to 850°C, having a decrease in LHV of the gas, from 13.15 to 9.34MJ/Nm³. The tar yield, had the same impact, going from 1.85g/Nm³ to 0.18g/Nm³. Another study, conducted by Hu et al., 2016 [60] of wet Sewage sludge and Pine sawdust, reached gasification temperature variation from 600 to 900°C a decrease in tar content from 15.34 to 2.19% by mass of gas, as well as a decrease of LHV from 12.32 to 10.65MJ/Nm³. According to [28], an increase in temperature enhance the tar-cracking reactions, producing H_2, CO, and CO_2.

4.3 Downdraft model

After the Pyrolysis analysis, the model was implemented for the Downdraft gasifier to analyze the Syngas produced, using the same Pyrolysis model.

The ER calculation was based on Rabea *et al.*, 2022 [64] equation, and it was considered the amount of oxygen in biomass, decreasing the necessity of air feed due to the presence of this component in the line "Char_cracking" after the Yield Reactor "Pyrolysis Char". Therefore, the ER varies depending on the amount of this component in the UA.

Results were considered based on the Syngas, dried, and free of nitrogen gas, which comes mainly from the "Air" line.

The Downdraft model was implemented for the biomasses chosen: Grape marc (GM), olive residue (OR), and corn straw (CS). To understand how the process behaves, the three biomasses were simulated, considering the same ER (0.36) and the same S/B ratio (0.42), which is available in Table 15 for each biomass, and then, the main lines were organized in Table 16, 17 and 18, being possible to verify the mole, temperature, and mass flow variation.

Table 15. Input conditions to the system.

	Biomass		
	Olive residue	Grape marc	Corn straw
ER (kg.air/h)	11.5	10.00	9.00
S/B ratio (kg.steam/h)	4.10	4.00	4.04

Table 16. Characteristics of main lines, in mole fraction, of grape marc (GM) simulation in Downdraft model.

	Mix	**Comb_top**	**Gas_top1**	**Gas_top2**	**Dried_Syngas**
H_2O	0.0357	0.0021	0.0146	0.0490	0.0000
CH_4	0.0064	0.0159	0.0648	0.0530	0.0746
C_6H_7	0.0105	0.0000	0.0000	0.0000	0.0000
C_6H_6	0.0370	0.0000	0.0000	0.0000	0.0000
O_2	0.1273	0.0000	0.0000	0.0000	0.0000
H_2	0.1729	0.3047	0.2619	0.3046	0.4284
$C_{(s)}$	0.1493	0.0000	0.0000	0.0000	0.0000
$S_{(s)}$	0.0002	0.0000	0.0000	0.0000	0.0001
CO	0.0527	0.3672	0.3525	0.2641	0.3715
CO_2	0.0458	0.0024	0.0352	0.0872	0.1227
N_2	0.3547	0.3053	0.2688	0.2402	0.0000
$C_{10}H_8$	0.0075	0.0024	0.0021	0.0019	0.0026
Mass Flow (kg/h)	19.62	18.22	21.62	23.62	14.88
Temperature (°C)	326.90	834.27	681.28	652.93	652.93
LHV (MJ/Nm³)					11.99
HHV (MJ/Nm³)					13.12

Table 17. Characteristics of main lines, in mole fraction, of olive residue (OR) simulation in Downdraft model.

	Mix	**Comb_top**	**Gas_top1**	**Gas_top2**	**Dried_Syngas**
H_2O	0.0326	0.0018	0.0123	0.0443	0.0000
CH_4	0.0059	0.0124	0.0625	0.0509	0.0730
C_6H_7	0.0096	0.0000	0.0000	0.0000	0.0000
C_6H_6	0.0340	0.0000	0.0000	0.0000	0.0000
O_2	0.1305	0.0000	0.0000	0.0000	0.0000
H_2	0.1545	0.2936	0.2496	0.2939	0.4218
$C_{(s)}$	0.1485	0.0000	0.0000	0.0000	0.0000
$S_{(s)}$	0.0002	0.0000	0.0000	0.0000	0.0002
CO	0.0484	0.3623	0.3552	0.2688	0.3857
CO_2	0.0421	0.0021	0.0309	0.0825	0.1184
N_2	0.3868	0.3270	0.2888	0.2590	0.0000
$C_{10}H_8$	0.0069	0.0008	0.0007	0.0006	0.0009
Mass Flow (kg/h)	21.18	19.66	23.23	25.28	15.45
Temperature (°C)	312.13	846.86	683.86	654.60	654.60
LHV (MJ/Nm³)					12.04
HHV (MJ/Nm³)					13.15

Table 18. Characteristic of main lines, in mole fraction, of corn straw (CS) simulation in Downdraft model

	Mix	**Comb_top**	**Gas_top1**	**Gas_top2**	**Dried_Syngas**
H_2O	0.0375	0.0019	0.0177	0.0551	0.0000
CH_4	0.0067	0.0163	0.0593	0.0483	0.0666
C_6H_7	0.0110	0.0000	0.0000	0.0000	0.0000
C_6H_6	0.0390	0.0000	0.0000	0.0000	0.0000
O_2	0.1314	0.0000	0.0000	0.0000	0.0000
H_2	0.1872	0.3183	0.2838	0.3225	0.4447
$C_{(s)}$	0.1417	0.0000	0.0000	0.0000	0.0000
$S_{(s)}$	0.0001	0.0000	0.0000	0.0000	0.0001
CO	0.0554	0.3762	0.3518	0.2623	0.3617
CO_2	0.0482	0.0021	0.0382	0.0899	0.1239
N_2	0.3338	0.2823	0.2466	0.2198	0.0000
$C_{10}H_8$	0.0079	0.0029	0.0025	0.0022	0.0031
Mass Flow (kg/h)	18.63	17.37	20.65	22.67	14.63
Temperature (°C)	338.26	844.10	686.13	657.55	657.54
LHV (MJ/Nm³)					11.75
HHV (MJ/Nm³)					12.88

The first observation of results is the similarity of the "Mix" line for the biomasses simulations. It is due to the second-order equations of the Pyrolysis process considering only the temperature as a variable, not counting the VM and FC, as well as other differences between biomasses, namely the amounts of Cellulose, Lignin, and Hemicellulose. Biomass lefts the Pyrolysis process at a temperature of 500°C, and is mixed with air, of line "Air" at 25°C, decreasing the temperature of line "Mix" to 326.90, 312.13, and 338.26°C, for grape marc, olive residue, and corn straw, respectively. It is interesting to note the bigger decrease in the OR temperature regarding GM, and CS, once that biomass needs more air given by the ER, which is at ambient temperature (25°C), supplied by the line "air". In turn, the mass flow follows the same behavior. In the combustion zone, the oxygen is completely consumed, as well as benzene and toluene through the reactions R(8) "Toluene oxidation" and R(9) "Benzene oxidation", elevating the temperature until 834.27, 846.86, and 844.10°C, respectively. Other points to consider in this zone, are the increase in CO, CH_4, and H_2 mole fractions, whereas H_2O and CO_2 mole fraction decrease. The mass flow in the first step of the reduction is incremented by the line "Steam1", which is at the temperature of 150°C, helping in a decrease in the temperature of the process, 681.28, 683.86, and 686.13°C, respectively. In the line, "Gas_top1", there is a high increase in the mole fraction of CH_4 and CO_2, while CO and H_2, decrease slightly. The increment in CH_4 mole fraction is given by the reaction R(12) "Hydrogasification". At the same time, the reaction R(11) "Carbon Reforming" is favored regarding R(10) "Boudouard Reaction" due to the less amount of energy necessary to happen, given by the enthalpy. In the second step of the Reduction zone, the "Gasification Homogeneous" reactor receives another line of steam "Steam2", increasing the mass flow, and decreasing the temperature of the system. Steam still favors increasing the amount of H_2 and CO_2 mole fractions, and decreasing CO and CH_4, once the reactions R(13) "Steam-methane Reforming" and R(14) "Water Gas Shift Reaction" tend to dislocate to the formation of the products, given the excess of water in the medium.

To facilitate the view of the main gases present in the line "Dried_Syngas" for each biomass, it is plotted in Figure 11, below.

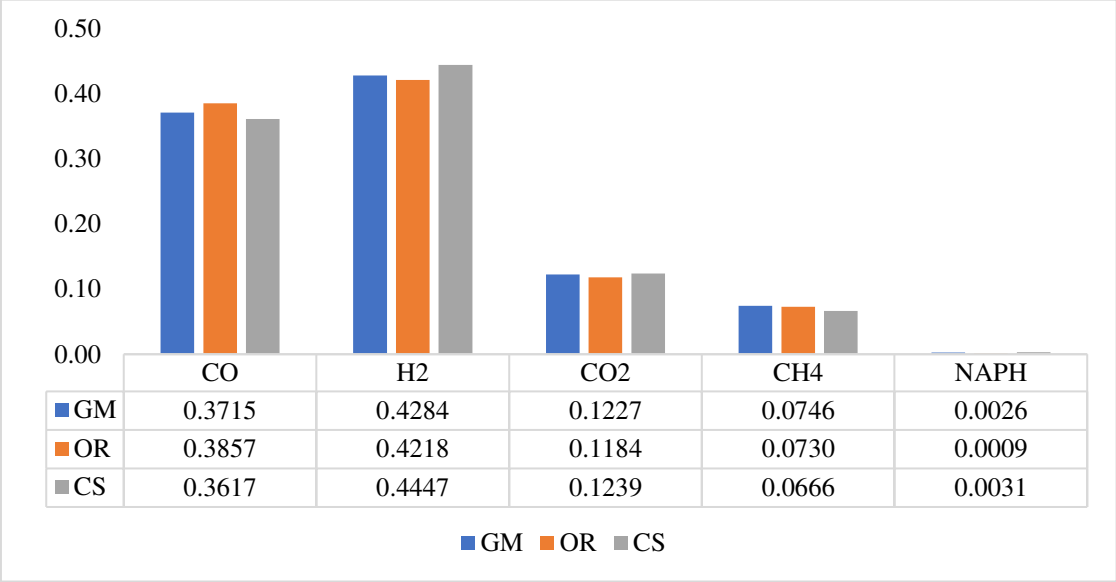

	CO	H2	CO2	CH4	NAPH
GM	0.3715	0.4284	0.1227	0.0746	0.0026
OR	0.3857	0.4218	0.1184	0.0730	0.0009
CS	0.3617	0.4447	0.1239	0.0666	0.0031

Figure 10. Main gases present in the line "Dried_Syngas" for each biomass.

It is possible to note the inverse proportionality between CO and CO_2 gases, which can be explained by the reaction "Water Gas Shift" in the last reactor of the Reduction zone "Gasification Homogeneous", as well as the direct proportionality between the amount of mass of hydrogen given by UA for each biomass with the amount that resulted from the simulation, having CS the biggest amount of H_2 in the Syngas, and hydrogen in UA, followed by GM, and OR. Another tendency noted is the direct proportionality between the amount of solid carbon and the CO produced, since, OR possesses the biggest amount of carbon in its biomass composition, which resulted in the biggest amount of CO in the Syngas produced, while GM is the second for both amounts and CS the third. In turn, CO_2 varies oppositely.

About the heating value, HHV in the line "Gas_top2" is smaller than the "Dried_Syngas" due to the dilution of the gas into non-fuel gases such as N_2 and H_2O. When this gas is cleaned in the last Separator of the simulation, the Syngas from GM and OR show higher values, once both have more or similar quantities of CH_4 in their composition, which has a greater influence on the heating value.

Tar, at the final of the process, is composed only of naphthalene, once benzene and toluene are all consumed in the Combustion zone. All biomasses produced low values of tar in the Syngas composition, having CS being the biggest amount, approximately 0.31, while GM has 0.26, and OR 0.09%, on a mole basis. The work conducted by Lv et al., 2007 [65], varying the ER from 0.22 to 0.26, and the S/B ratio from 0.32 to 0.69, reached values, in volume fraction, for tar in the Syngas composition, from 0.27% to 1.30%. According to the literature [26], the maximum limit considered for tar composition in Syngas is 0.1g/Nm³, being the results of simulation high above this value, 6.8, 2.4, 8.2g/Nm³ in the line "Crude_Syngas", for GM, OR,

CS, respectively. However, many works reported tar concentrations similar to this work. For instance, using Sawdust as biomass, Updraft gasifier, and air as the gasifying agent, Wang et al., 2011 [66], reached 8g/Nm³ of tar in Syngas composition, while Dogru et al., 2002 [67], employed a Hazelnut shell as biomass in a Downdraft gasifier, supplied by air, resulting in a tar composition of 3.3g/Nm³. A point to be considered in this model, is the high molecular weight of naphthalene, increasing the tar mass fraction content.

Some results of Syngas composition on a volume basis are shown in Table 19, below. Among them, the prediction and optimization of Syngas production based on a kinetic model, presented by Dang et al. [68], 2021, reached optimal ER = 0.32 and S/B ratio = 0.45, for a volume basis, using a Wood Residue (WR) as biomass. In another work, conducted by Oni et al., 2021 [69], with *Cymbopogon citratus* (CC) and Ni/dolomite/CeO_2/K_2CO as a catalyst, obtained the parameters ER = 0.27 and S/B ratio = 0.5. Lv et al., 2007 [65], in a very similar work, conducted in a lab scale laboratory for H_2-rich gas production in a Downdraft gasifier, using Pine wood (PW) as biomass, reported optimal ER = 0.24 and S/B ratio = 0.61.

Table 19. Comparison between the Biomasses tested in this work with biomasses tested in the literature.

	GM		OR		CS		WR		CC		PW	
	ER (0.36)	S/B (0.42)	ER (0.36)	S/B (0.42)	ER (0.36)	S/B (0.42)	ER (0.32)	S/B (0.45)	ER (0.27)	S/B (0.50)	ER (0.24)	S/B (0.61)
CO	0.36		0.37		0.36		0.28		0.26		0.39	
H_2	0.34		0.34		0.35		0.27		0.48		0.29	
CO_2	0.18		0.17		0.18		0.35		0.18		0.25	
CH_4	0.11		0.11		0.09		0.09		0.08		0.06	
Tar	0.009		0.003		0.01		-		-		0.01	
H_2/CO	0.94		0.92		0.97		0.96		1.88		0.74	
HHV (MJ/Nm³)	13.12		13.15		12.88		10.56		12.58		11.10	
Reference							[68]		[69]		[65]	

It is complex to compare results considering different gasification works. This is due to the fact that some works test the Syngas production in a real system, considering all the physical-chemical phenomena that take place inside the gasifier. On the other hand, different simulation studies use diverse modeling strategies, considering different reactions for each zone of the gasifier, as well as the different model types, which can be kinetic, equilibrium, and CFD models, generating distinct results, through the calculation on software platforms. In this model, for instance, the use of the Gibbs reactor in the combustion zone resulted in the low

formation of CO_2, compared with other works, a situation explained by the equilibrium reactions happening simultaneously, tending to increase CO instead of CO_2. The biomasses as much as their UA and PA compositions influence directly the results through different analyses. Anyway, the results achieved in this work show certain similarities, regarding the compositions, as well as HHV, for different ER and S/B ratio values.

4.3.1 ER variation

The Downdraft model was simulated considering the determination of the S/B ratio in (0.42), and varying ER in the interval from 0.23 to 0.54, for each biomass. Then, it is possible to analyze how the system interacts with the biomass under different conditions. Below, in Table 20, the maximum and minimum Airflow for each biomass are presented.

Table 20. Airflow variation for each biomass, into the interval (0.23–0.54).

		Biomass		
		Olive residue	Grape marc	Corn straw
ER (kg.air/h)	Maximum	24.0	22.0	22.0
	Minimum	2.0	1.5	0

To facilitate the visualization, the results were plotted in graphs given in Figures 11 and 12, regarding the variation in CO, H_2, CO_2, CH_4 mole fraction; HHV and LHV; and H_2/CO ratio. All results are based on Dried_Syngas, with no N_2.

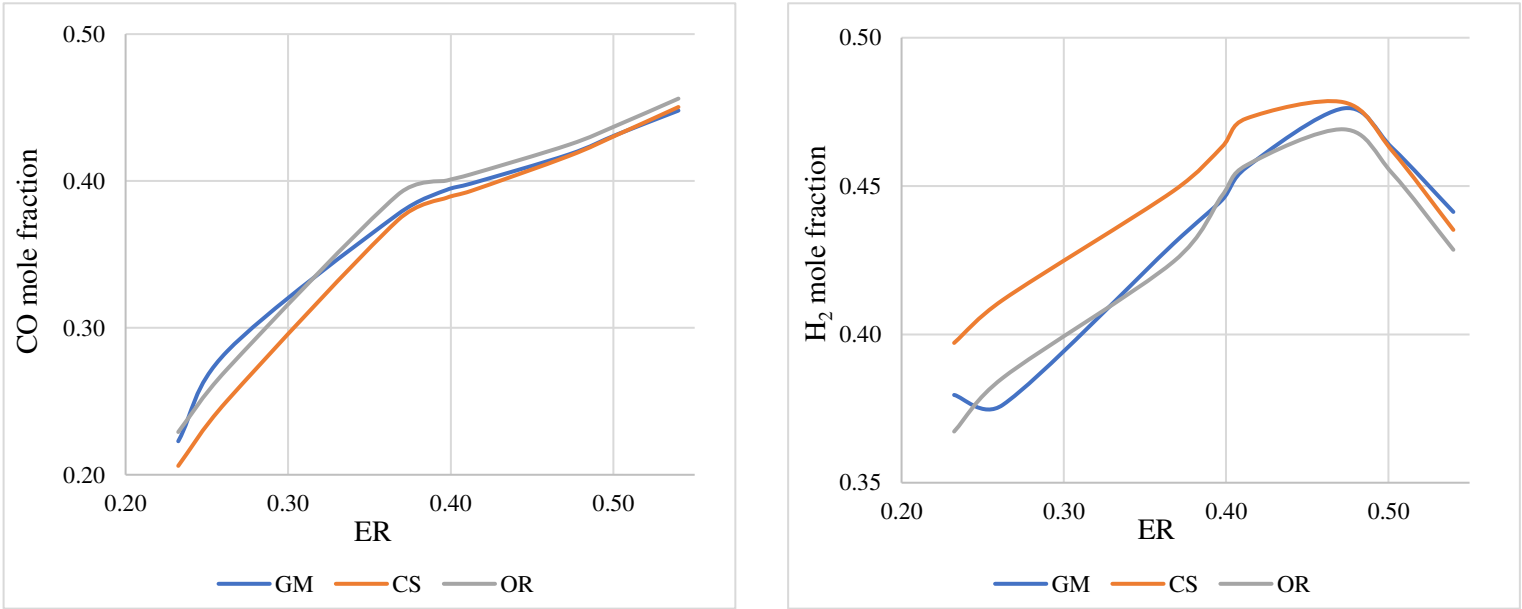

Figure 11. Component mole fraction for CO and H_2 in the line "Dried_Syngas", in sequence, versus ER variation.

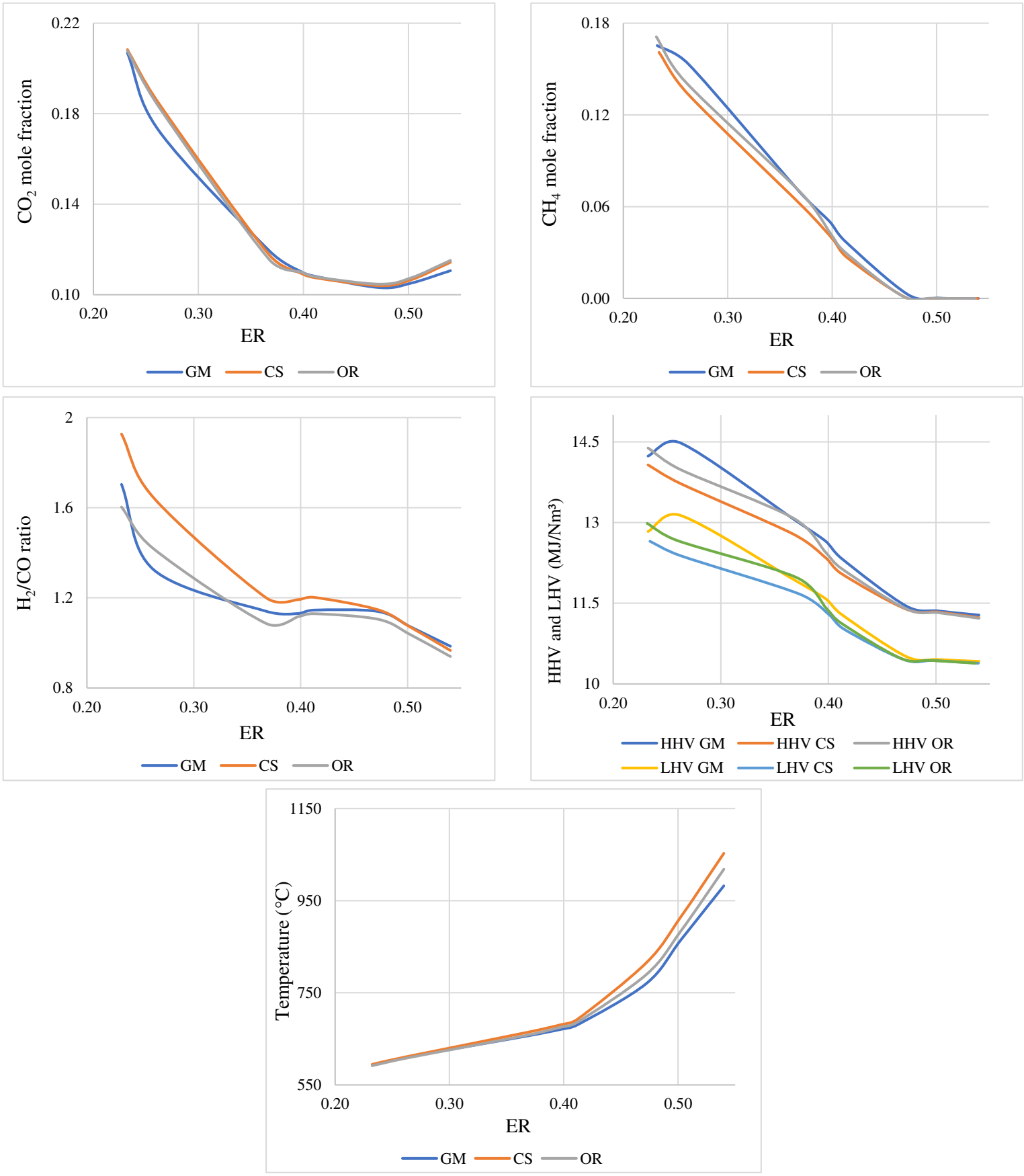

Figure 12. CO_2 and CH_4 mole fraction, ratio between hydrogen and carbon monoxide, HHV and LHV, and temperature (°C) of the line "Dried_Syngas", versus ER variation.

Concerning the quantities produced by each biomass, below, Table 21 shows the syngas compositions for the minimum ER (0.23), maximum ER (0.54), and the variation (δ), positive in green, or negative in red.

Table 21. Mole fraction of main components in the line "Dried_Syngas", considering the minimum and maximum ER points.

	GM			CS			OR		
	0.23	**0.54**	**δ**	**0.23**	**0.54**	**δ**	**0.23**	**0.54**	**δ**
CO	0.2228	0.4479	2.01	0.2061	0.4504	2.19	0.2291	0.4561	1.99
H_2	0.3796	0.4413	1.16	0.3971	0.4352	1.10	0.3673	0.4285	1.17
CO_2	0.2069	0.1106	0.46	0.2084	0.1143	0.45	0.2078	0.1152	0.45
CH_4	0.1654	0	1.00	0.1610	0	1.00	0.1711	0	1.00
NAPH	0.0251	0	1.00	0.0274	0	1.00	0.0244	0	1.00
H_2/CO	1.7035	0.9850	0.42	1.9270	0.9663	0.50	1.6031	0.9396	0.41
LHV (MJ/Nm³)	12.83	10.42	0.19	12.65	10.38	0.18	12.99	10.38	0.20
HHV (MJ/Nm³)	14.24	11.28	0.21	14.07	11.23	0.20	14.39	11.22	0.22
Temperature (°C)	593.47	982.13	1.65	594.70	1052.70	1.77	591.75	1018.15	1.72

4.3.1.1 System Behavior under ER variation

Through the plots presented, is possible to see the same behavior for all biomasses when the airflow is varied. Nevertheless, some differences, such as the amount of each component (CO, H_2, CO_2, CH_4), can be seen and analyzed. Carbon monoxide presents a comportment of fast-rising until approximately the ER point 0.37, which is due to the high amount of CO_2 converted through the Boudouard Reaction, until the point that most of the carbon is consumed, decreasing the rate of increase. The opposite is seen in the third graph, where the CO_2 mole fraction decreases quickly until the same point, and then the falling ratio decreases, starting to increase after the point 0.48. About H_2, the tendency is to rise until the 0.48 ER ratio point, when it starts to fall, due to the consumption of approximately all CH_4. On the opposite way, the CH_4 mole fraction goes down quickly, until reaches values near 0, at the same point as ER (0.48). The temperature at the final of the process, in line "Dried_Syngas," increases as ER rises, but there is an increment, around point 0.42, where the rising is more accentuated. These changes are explained by the reactions, once the increase in the ER favors an increment in the process temperature due to the total oxidation, which releases more heat since the reactions in the Combustion zone are exothermic. However, in the Reduction zone, R(11) "Carbon Reforming", R(10) "Boudouard Reaction" and R(13) "Steam-methane Reforming" are

endothermic, ceasing a fast-rising in temperature. When CH_4 is almost all consumed by R(13), and there is a lot of CO present in the medium, R(14) "Water Gas Shift Reaction", which is exothermic, is favored, consuming the CO, and increasing the rate of increase in system temperature. HHV and LHV decrease whereas CH_4 is consumed until CO becomes to be the highest influence in LHV, making the fall less abrupt. For HHV, in turn, H_2 has more impact, decreasing the value at a higher rate.

About the H_2/CO ratio, CS presents high superiority at the beginning while this decreases as the ER increases. The line presents the trend of falling, once the CO mole fraction has a steeper rise than H_2. Due to having a bigger amount of CH_4, than other biomasses, GM possesses an HHV more elevated, which decreases for all biomasses, following the CH_4 falling. To the Tar amount present in the Syngas, composition, the consumption of all naphthalene, the residual molecule of Tar, is made about the ER interval of 0.36–0.37. However, the peak for the H_2 mole fraction for OR is at ER 0.45 (0.4717), for GM is ER 0.46 (0.4771) and for CS is also ER 0.46 (0.4838). This peak position is very close to the expected from the literature, where the optimum ER, considering the maximum amount of H_2, is inside the interval of 0.2 and 0.4 [70].

In their study, Ibrahim et al., 2022 [71] tested an equilibrium model of a downdraft gasifier, with rubberwood as a carbon source, and moisture content at 18.5%. When analyzing the ER variation into the interval of 0.2–0.4, the diluted (summed with N_2 gas) Syngas demonstrated the same behavior, decreasing H_2, CO_2, and CH_4 mole fractions, while the CO mole fraction rises. In turn, Yan et al., 2018 [72], developed a thermal-equilibrium model-based, simulating a Downdraft gasifier in a CFD ambient, testing an ER variation between 0.2–0.4, and obtaining as result the increase in CO mole fraction, while H_2, CO_2, CH_4, and tar decrease for higher ER. Yu and Smith, 2018 [73], compared in their work two gasification models based on the Reaction kinetics model, and the Gibbs Free Energy model, resulting in very similar behavior for the second one when varied the ER from 0.10 to 0.30. CO and H_2 volume fraction increases, while CH_4 and CO_2 decrease as higher ER. Treating the mole fraction results, H_2 is the most distinct, concerning quantities, among the biomasses. CS has the highest amount of H_2, while GM and OR alternate with similar amounts during the simulation. Watson et al., 2018 [28], commented that CO and H_2 content initially increase, increasing the ER, and after, start to decrease, while CH_4 continuously decreases, and CO_2, in turn, increases, because more complete combustion reactions occur.

4.3.2 S/B ratio variation

In the same way as the last topic, the Downdraft model was simulated considering the determination of the ER ratio in (0.36), and varying the S/B ratio between the interval from 0 to 1, for each biomass. Then, it is possible to analyze how the system interacts with the biomass under different conditions. The maximum and minimum steam flow for each biomass are presented in Table 22.

Table 22. Steam flow variation for each biomass, in the interval (0–1).

		Biomass		
		Olive residue	Grape marc	Corn straw
S/B ratio (kg.steam/h)	Maximum	9.86	9.62	9.63
	Minimum	0	0	0

To facilitate the visualization, the results were plotted in graphs given in Figures 13 and 14, being them: CO, H_2, CO_2, CH_4 mole fraction; HHV and LHV; and H_2/CO ratio. All results are based on Dried_Syngas, with no N_2.

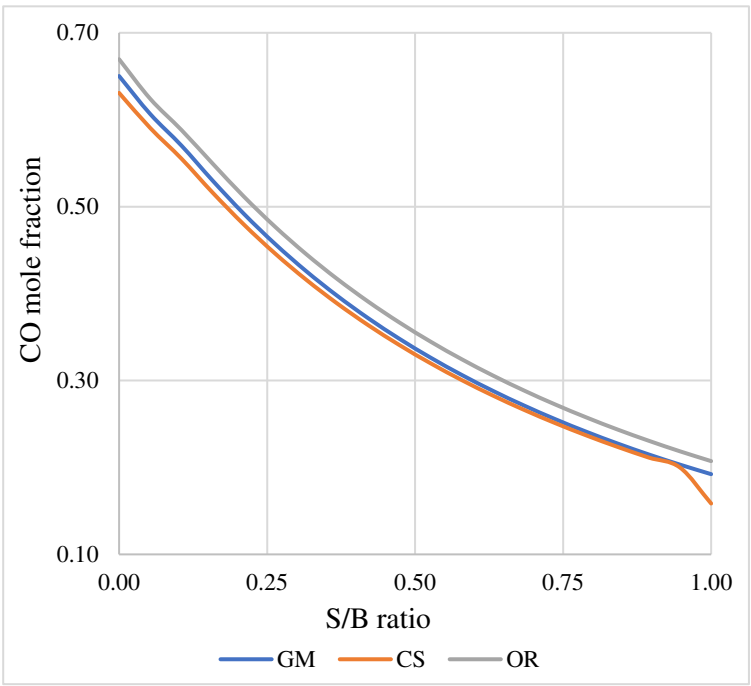

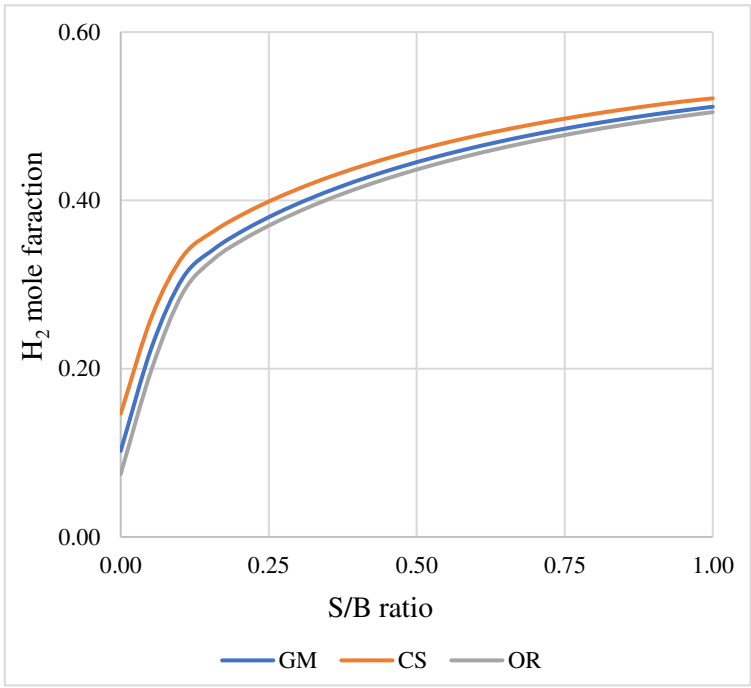

Figure 13. Component mole fraction for CO and H_2 in the line "Dried_Syngas", in sequence, versus S/B ratio variation.

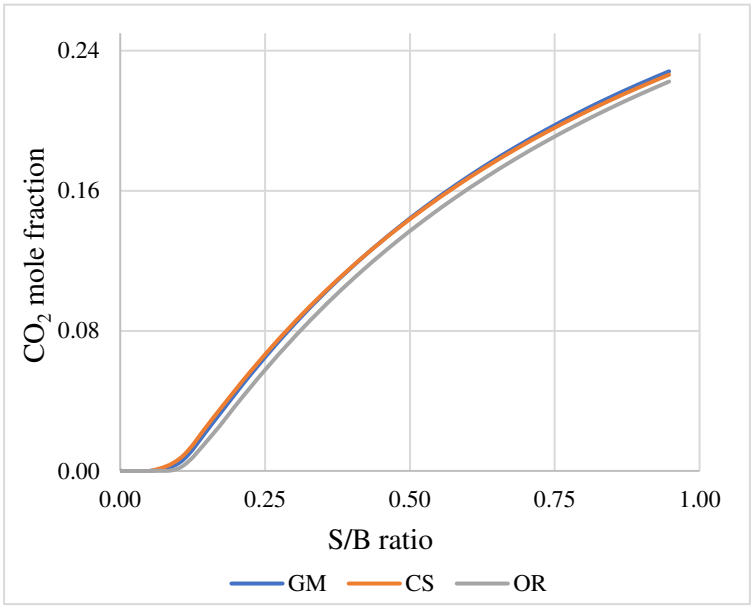

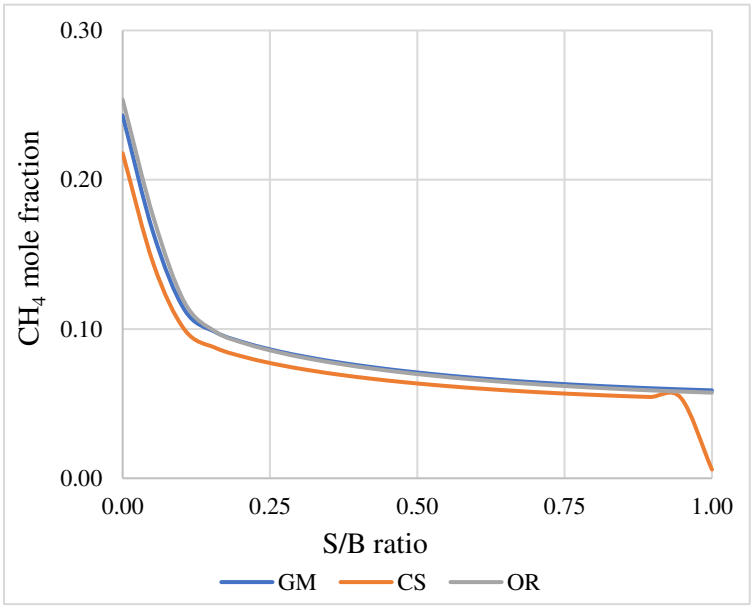

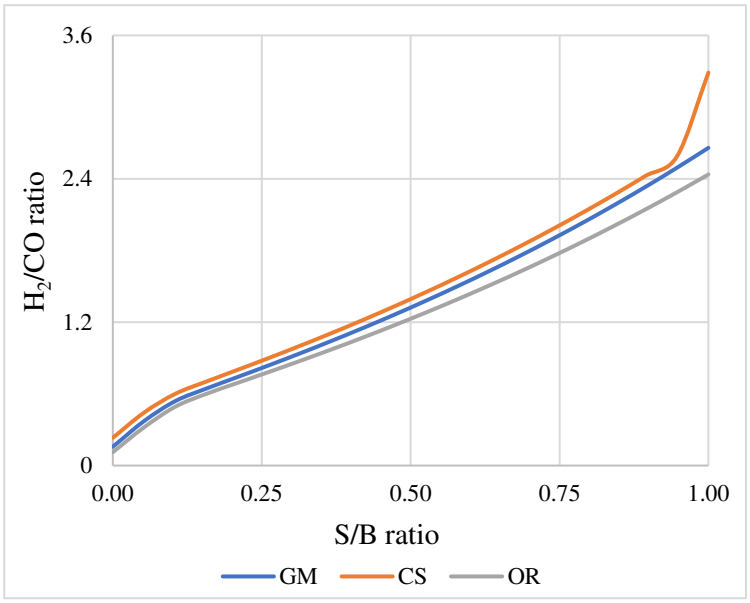

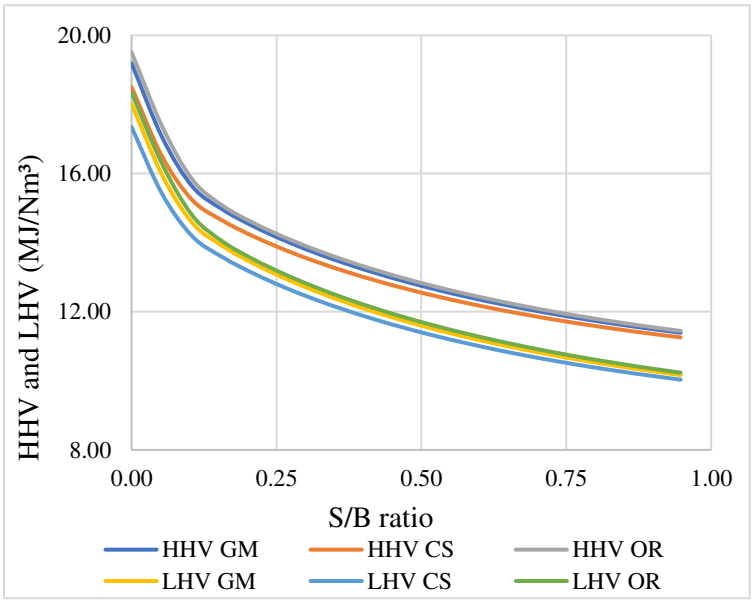

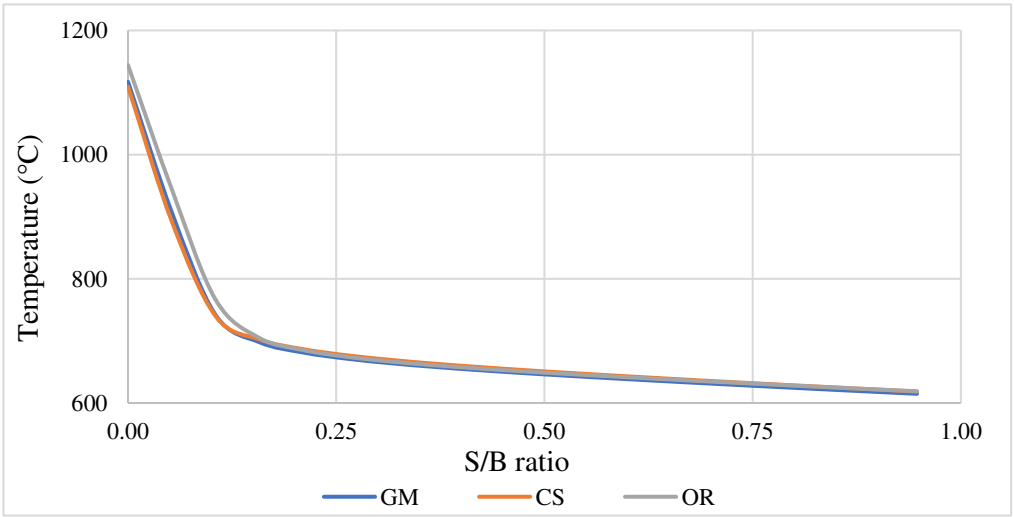

Figure 14. CO_2 and CH_4 mole fraction, ratio between hydrogen and carbon monoxide, HHV and LHV, and temperature of the line "Dried_Syngas", versus S/B ratio variation.

Concerning the quantities produced by each biomass, below, Table 23 shows the syngas compositions for minimum S/B ratio (0), maximum S/B ratio (0.95), and the variation (δ), positive in green, or negative in red.

Table 23. Mole fraction of main components in the line "Dried_Syngas", considering the minimum and maximum S/B ratio points.

	GM			CS			OR		
	0	**0.95**	**δ**	**0**	**0.95**	**δ**	**0**	**0.95**	**δ**
CO	0.6503	0.2032	0.69	0.6309	0.1999	0.68	0.6696	0.2186	0.67
H_2	0.1024	0.5066	4.95	0.1466	0.5173	3.53	0.0749	0.5000	6.67
CO_2	0	0.2282	-	0	0.2263	-	0	0.2224	0.45
CH_4	0.2430	0.0596	0.75	0.2178	0.0538	0.75	0.2537	0.0581	0.77
NAPH	0.0041	0.0023	0.45	0.0047	0.0027	0.43	0.0015	0.0008	0.46
H_2/CO	0.1574	2.4927	15.84	0.2323	2.5874	11.14	0.1119	2.2873	20.44
LHV (MJ/Nm³)	18.02	10.17	0.44	17.35	10.03	0.42	18.35	10.24	0.44
HHV (MJ/Nm³)	19.19	11.39	0.41	18.51	11.26	0.39	19.51	11.44	0.41
Temperature (C°)	1117.34	614.77	0.45	1109.49	618.43	0.44	1144.22	618.82	0.46

4.3.2.1 System behavior under S/B ratio variation

According to the simulations, varying the S/B ratio, the mole fractions of each biomass component exhibit similar behavior. Carbon monoxide decreases as the S/B ratio increases, being a result of the R(14) "Water Gas Shift Reaction", which increases CO_2 and H_2 mole fraction. In turn, the H_2 mole fraction is also incremented by the consumption of CH_4, through the reaction R(13) "Steam-methane Reforming". It is possible to note the preference of R(13) in relation to R(14) at the beginning of the S/B ratio variation, when, next to the point (0.1), after the high consumption of CH_4, there is a "brake", increasing CO_2 mole fraction through R(14). This high consumption of CH_4 decreases the temperature very fast, which could be seen in both graphs, at the point S/B ratio 0.12, where the decrease in temperature starts to be slower. The low initial value of CO_2 mole fraction is explained because of the consumption generated by the R(10) "Boudouard Reaction" which consumes the solid carbon and CO_2, favoring the increase in CO mole fraction. The HHV and LHV follow the CH_4 behavior, once this component has the highest weight considering the calorific power. Tar mole fraction is not affected in this model by the S/B ratio, being the last value not as low than the first because of the dilution caused by the increment of steam in the mass flow. The mole fraction of H_2 in the Syngas follows the amount of hydrogen in the UA composition. In this way, CS which possesses the larger amount of hydrogen given by UA also produced Syngas with the highest

amount of this component in the simulation (0.5173). Next, GM, the biomass with the second higher hydrogen quantity in its UA composition, produced Syngas with 0.5066 of H_2, and finally, OR produced Syngas with 0.5000 of hydrogen gas, on a mole fraction basis. The same trend is seen for the solid carbon component given by UA for each biomass, and CO mole fraction in the Syngas composition, having OR the highest amount of solid carbon, followed by GM and CS. The results are shown in Table 23, where OR has 0.2186 of CO mole fraction in the Syngas composition, while GM has 0.2032, and CS has 0.1999. All results consider the last point of the S/B ratio (0.95).

About the H_2/CO ratio, it increases for all the S/B ratio variations, since the CO mole fraction falls, while the H_2 mole fraction increases.

Ghorbani et al., 2022 [74], using a kinetic model for Pyrolysis based on lignocellulosic biomass composition, tested the effect of moisture content in the Syngas produced by a Downdraft biomass gasification process, concluding that for higher moisture contents, the mole fraction of CO and CH_4 decrease, while CO_2 and H_2 increase, having the last one a reduction in the rate of rising. Another work presented by Kakati et al., 2022 [75], using bamboo as a biomass source in an air-steam medium in a Downdraft gasifier, and a variation from 0.1 to 0.4 in S/B ratio, reached an increase of H_2 and CO_2 mole fractions, while CH_4 and CO reduce as S/B increases. Varying the moisture content between the interval of 0 to 25% by mass, Tauqir et al., 2019 [76], concluded that for higher moistures, the H_2/CO ratio increased, as well as the LHV decreased. Garcia et al., 1999 [77], reported in their work that the increase in the S/B ratio, causes the surge in H_2 and CO_2 mole fractions, while CO and CH_4 decrease. This is corroborated by Hernandez et al., 2012 [78], which studied grape marc gasification. For higher S/B ratios, the larger is H_2/CO, while the lower appears to be the CH_4/H_2 ratio. Another study, conducted by Wang et al., 2018 [28], shows a big decrease in LHV from 13.62 to 9.40MJ/Nm³, increasing the S/B ratio from 0 to 3.08, while tar decreases from 40.15g/Nm³ until S/B ratio 1.23, when starts to increase, reaching at the point 3.08 in 2.86g/Nm³. The same trend is seen in Doherty et al., 2009 [79] work which added steam in a Circulating Fluidised bed reactor, simulated in Aspen Plus, using Hemlock wood as biomass, resulting in a slight drop of HHV from 4.69 to 4.62MJ/Nm³, for larger quantities of injected steam. Hydrogen gas composition still increased from 13.7 to 16.7% on a mole basis, as well as CO_2, while CO and CH_4 decreased.

5 CONCLUSIONS

The second-order model chosen for the Pyrolysis process has some similarities and variations when compared with the literature, showing Gas, Tar, and Char values and variations with temperature following other works [55][56]. The results of the Pyrolysis model applied in the simulation showed similarities with literature for CH_4, H_2, Tar, and Char, while CO and CO_2 showed some variation [57][58][59]. The limitation of the model relates to the consideration of the temperature as the only variable, exhibiting similar results for different biomasses.

The Downdraft gasifier simulated based on the second-order Pyrolysis model showed similar results compared with the literature [65][68][69]. Some variations in Syngas composition, as well as the CO mole fraction and H_2 mole fraction followed the UA compositions of biomasses, considering solid carbon and hydrogen, respectively.

Applying the Gibbs reactor in the combustion zone decreased the CO_2, once the equilibrium tended to produce more of the CO component, becoming the carbon dioxide result underestimate. A good point is the inclusion of two Gibbs reactors in the Reduction zone, enabling the utilization of all necessary equilibrium reactions, as well as the feeding with two streams of steam, which reach the reactors at the same temperature and conditions. The combustion zone can be reviewed to reach stoichiometric values for the reactions, allowing the utilization of a Conversion reactor.

Based on the literature, the fall of tar and CH_4 is common, as the higher ER, while CO, CO_2, and H_2 show distinct behaviors depending on the model and conditions applied [71][72][73]. Regarding S/B ratio variation, there is a similarity with the literature [74][75][77][78][79] in the increase of H_2 and CO_2 mole fractions, as higher the S/B ratio, while CO and CH_4 decreases, explained by the Steam-methane Reforming and Water Gas Shift Reactions. CS showed up to be, in both simulations (ER and S/B ratio), the H_2-richer Syngas producer biomass, while OR is the poorest in this component. Toluene and benzene are all consumed by the Combustion zone, while naphthalene remains in the process, which can be related to the molecule conformation, having the last one more unsaturated links, due to the presence of two aromatic rings, becoming the consumption harder. Naphthalene suffered a strong impact, increasing ER, while the S/B ratio does not affect its composition.

An increase in ER has a significant impact on the increase of H_2 and CO mole fractions, and temperature, while Tar, CH_4, CO_2, H_2/CO, HHV, and LHV are impacted negatively. The greatest point, considering the Syngas standard high-quality is around 0.46 and 0.47 where the

mole fraction of H_2 for CS is the biggest (0.48). Considering the S/B ratio variation, the increase in this parameter, varied highly in CO_2 amount, as well as increased H_2 mole fraction, and consequently H_2/CO ratio. Negatively affected, the CO and CH_4 mole fraction, LHV, HHV, and temperature, while Tar was not affected by the steam variation. The biomass which presented the highest amount of H_2 is again CS (0.52), but there is still an opportunity to increase, once the H_2 curve is still rising. All biomasses presented a similar trend for each component of Syngas when the ER and S/B ratios were increased.

For future works, a modification can be applied, adding to the second-order model a weighted model, based on the literature, differing the amount of VM and FC for each biomass in order to ponder the amount of Gas, Tar, and Char, which will be produced in the Pyrolysis process. The combustion process can be improved by employing a conversion or kinetic reactor and collecting data from literature about yields achieved in reactions in this step. Another improvement is to link the energy lines of the process, in order to make it energetically self-sustaining, and verify its economic viability. Carbon dioxide produced in the process can be reintroduced in the reduction zone to analyze carbon monoxide variations, in an attempt of improving the process efficiency.

6 REFERENCES

[1] M. Abreu et al., “Evaluation of the Potential of Biomass to Energy in Portugal—Conclusions from the CONVERTE Project,” *Energies 2020*, vol. 13, pp. 937, Feb. 2020, doi: 10.3390/EN13040937.

[2] S. Ferreira, E. Monteiro, P. Brito, and C. Vilarinho, “Biomass resources in Portugal: Current status and prospects,” *Renew. Sustain. Energy Rev.*, vol. 78, pp. 1221-1235, Oct. 2017, doi: 10.1016/J.RSER.2017.03.140.

[3] P. Basu, “Biomass Gasification and Pyrolysis,” *Biomass Gasif. Pyrolysis*, pp. 1-365, 2010, Elsevier Inc., doi: 10.1016/C2009-0-20099-7.

[4] S. V. Vassilev et al., “An overview of the chemical composition of biomass,” *Fuel*, vol. 89, no. 5, pp. 913-933, May 2010, doi: 10.1016/J.FUEL.2009.10.022.

[5] P. Basu, “Biomass Gasification, Pyrolysis and Torrefaction: Practical Design and Theory,” Biomass Gasification, Pyrolysis Torrefaction Pract. Des. Theory, pp. 1-530, second edition, 2013, Elsevier Inc., doi: 10.1016/C2011-0-07564-6.

[6] S. Pang, “Advances in thermochemical conversion of woody biomass to energy, fuels and chemicals,” *Biotechnol. Adv.*, vol. 37, no. 4, pp. 589-597, Jul. 2019, doi: 10.1016/J.BIOTECHADV.2018.11.004.

[7] C. Font Palma, “Modelling of tar formation and evolution for biomass gasification: A review,” *Appl. Energy*, vol. 111, pp. 129-141, Nov. 2013, doi: 10.1016/J.APENERGY.2013.04.082.

[8] A. Frassoldati and E. Ranzi, “Modeling of Thermochemical Conversion of Biomasses,” *Ref. Modul. Chem. Mol. Sci. Chem. Eng.*, Jan. 2019, doi: 10.1016/B978-0-12-409547-2.11625-7.

[9] S. Li et al., “CO_2 gasification of straw biomass and its correlation with the feedstock characteristics,” *Fuel*, vol. 297, pp. 120780, Aug. 2021, doi: 10.1016/J.FUEL.2021.120780.

[10] Y. H. Qin, A. Campen, T. Wiltowski, J. Feng, and W. Li, “The influence of different chemical compositions in biomass on gasification tar formation,” *Biomass and Bioenergy,* vol. 83, pp. 77-84, Dec. 2015, doi: 10.1016/J.BIOMBIOE.2015.09.001.

[11] S. Gaur and T. B. Reed, "Overview of Thermal Analysis Methods", *Thermal data for natural and synthetic fuels*, pp. 18-19, First edition, 1998, Marcel Dekker, Inc., doi:

10.1201/9781003064633

[12] J. Dai, J. Saayman, J. R. Grace, and N. Ellis, “Gasification of Woody Biomass,” *Annual Review of Chemical and Biomolecular Engineering*, vol. 6, pp. 77-99, Aug. 2015, doi: 10.1146/ANNUREV-CHEMBIOENG-061114-123310.

[13] M. Bassyouni *et al.*, “Date palm waste gasification in downdraft gasifier and simulation using ASPEN HYSYS,” *Energy Convers. Manag.*, vol. 88, pp. 693-699, Dec. 2014, doi: 10.1016/J.ENCONMAN.2014.08.061.

[14] C. Wu, Z. Wang, J. Huang, and P. T. Williams, “Pyrolysis/gasification of cellulose, hemicellulose and lignin for hydrogen production in the presence of various nickel-based catalysts,” *Fuel*, vol. 106, pp. 697-706, Apr. 2013, doi: 10.1016/J.FUEL.2012.10.064.

[15] S. Maisano et al., “Syngas production by BFB gasification: Experimental comparison of different biomasses,” *Int. J. Hydrogen Energy*, vol. 44, pp. 4414-4422, Feb. 2019, doi: 10.1016/J.IJHYDENE.2018.11.148.

[16] T. Tian *et al.*, “Effects of biochemical composition on hydrogen production by biomass gasification,” *Int. J. Hydrogen Energy*, vol. 42, no. 31, pp. 19723-19732, Aug. 2017, doi: 10.1016/J.IJHYDENE.2017.06.174.

[17] M. Mehrpooya, M. Khalili, and M. M. M. Sharifzadeh, “Model development and energy and exergy analysis of the biomass gasification process (Based on the various biomass sources),” *Renew. Sustain. Energy Rev.*, vol. 91, pp. 869-887, Aug. 2018, doi: 10.1016/J.RSER.2018.04.076.

[18] N. Couto *et al.*, “Influence of the Biomass Gasification Processes on the Final Composition of Syngas,” *Energy Procedia*, vol. 36, pp. 596-606, Jan. 2013, doi: 10.1016/J.EGYPRO.2013.07.068.

[19] A. Demirbaş, “Biomass resource facilities and biomass conversion processing for fuels and chemicals,” *Energy Convers. Manag.*, vol. 42, no. 11, pp. 1357-1378, Jul. 2001, doi: 10.1016/S0196-8904(00)00137-0.

[20] H. Liu *et al.*, “Three-dimensional full-loop simulation of a dual fluidized-bed biomass gasifier,” *Appl. Energy*, vol. 160, pp. 489-501, Dec. 2015, doi: 10.1016/J.APENERGY.2015.09.065.

[21] T. Chen, T. Li, J. Sjöblom, and H. Ström, “A reactor-scale CFD model of soot formation

during high-temperature pyrolysis and gasification of biomass," *Fuel*, vol. 303, pp. 121240, Nov. 2021, doi: 10.1016/J.FUEL.2021.121240.

[22] A. Porcu *et al.*, "Experimental validation of a multiphase flow model of a lab-scale fluidized-bed gasification unit," *Appl. Energy*, vol. 293, no. C, pp. 116963, Jul. 2021, doi: 10.1016/J.APENERGY.2021.116933.

[23] N. Gao and A. Li, "Modeling and simulation of combined pyrolysis and reduction zone for a downdraft biomass gasifier," *Energy Convers. Manag.*, vol. 49, no. 12, pp. 3483-3490, Dec. 2008, doi: 10.1016/J.ENCONMAN.2008.08.002.

[24] A. S. Al-Rahbi and P. T. Williams, "Hydrogen-rich syngas production and tar removal from biomass gasification using sacrificial tyre pyrolysis char," *Appl. Energy*, vol. 190, pp. 501-509, Mar. 2017, doi: 10.1016/J.APENERGY.2016.12.099.

[25] M. Puig-Gamero *et al.*, "Simulation of biomass gasification in bubbling fluidized bed reactor using aspen plus®," *Energy Convers. Manag.*, vol. 235, pp. 113981, May 2021, doi: 10.1016/J.ENCONMAN.2021.113981.

[26] S. Mishra and R. K. Upadhyay, "Review on biomass gasification: Gasifiers, gasifying mediums, and operational parameters," *Mater. Sci. Energy Technol.*, vol. 4, pp. 329-340, Jan. 2021, doi: 10.1016/J.MSET.2021.08.009.

[27] M. M. Parascanu *et al.*, "Valorization of Mexican biomasses through pyrolysis, combustion and gasification processes," *Renew. Sustain. ENERGY Rev.*, vol. 71, pp. 509-522, May 2017, doi: 10.1016/j.rser.2016.12.079.

[28] J. Watson *et al.*, "Gasification of biowaste: A critical review and outlooks," *Renew. Sustain. Energy Rev.*, vol. 83, pp. 1-17, Mar. 2018, doi: 10.1016/J.RSER.2017.10.003.

[29] V. Kirubakaran *et al.*, "A review on gasification of biomass," *Renew. Sustain. Energy Rev.*, vol. 13, no. 1, pp. 179-186, Jan. 2009, doi: 10.1016/J.RSER.2007.07.001.

[30] T. Damartzis, S. Michailos, and A. Zabaniotou, "Energetic assessment of a combined heat and power integrated biomass gasification–internal combustion engine system by using Aspen Plus®," *Fuel Process. Technol.*, vol. 95, pp. 37-44, Mar. 2012, doi: 10.1016/J.FUPROC.2011.11.010.

[31] M. Asadullah, "Barriers of commercial power generation using biomass gasification gas: A review," *Renew. Sustain. Energy Rev.*, vol. 29, pp. 201-215, Jan. 2014, doi: 10.1016/J.RSER.2013.08.074.

[32] A. A. Ahmad *et al.*, "Assessing the gasification performance of biomass: A review on biomass gasification process conditions, optimization and economic evaluation," *Renew. Sustain. Energy Rev.*, vol. 53, pp. 1333-1347, Jan. 2016, doi: 10.1016/J.RSER.2015.09.030.

[33] D. S. Barriquello, "Análise econômica e ambiental de processo de produção de gás de síntese a partir de biomassa algal.", *Masters dissertation, Universidade Federal do Rio de Janeiro*, pp. 20, Jan. 2013, Acessed: http://www.h2cin.org.br/download/gas-de-sintese-a-partir-de-biomassa-algal.pdf

[34] A. Chanthakett *et al.*, "Performance assessment of gasification reactors for sustainable management of municipal solid waste," *J. Environ. Manage.*, vol. 291, pp. 112661, Aug. 2021, doi: 10.1016/J.JENVMAN.2021.112661.

[35] E. Tool Box, "Combustion Heat," *Resources, Tools and Basic Information for Engineering and Design of Technical Applications!*, 2017, Acessed: https://www.engineeringtoolbox.com/standard-heat-of-combustion-energy-content-d_1987.html

[36] J. Yu *et al.*, "A review of the effects of alkali and alkaline earth metal species on biomass gasification," *Fuel Process. Technol.*, vol. 214, pp. 106723, Apr. 2021, doi: 10.1016/J.FUPROC.2021.106723.

[37] S. Karimipour *et al.*, "Study of factors affecting syngas quality and their interactions in fluidized bed gasification of lignite coal," *Fuel Process. Technol.*, vol. 103, pp. 308-320, Jan. 2013, doi: 10.1016/j.fuel.2012.06.052.

[38] J. Zeng, R. Xiao, and J. Yuan, "High-quality syngas production from biomass driven by chemical looping on a PY-GA coupled reactor," *Energy*, vol. 214, pp. 118846, Jan. 2021, doi: 10.1016/J.ENERGY.2020.118846.

[39] Z. Liu, C. Zhao, L. Cai, and X. Long, "Steady state modelling of steam-gasification of biomass for H_2-rich syngas production," *Energy*, vol. 238, pp. 121616, Jan. 2022, doi: 10.1016/J.ENERGY.2021.121616.

[40] M. Hussain *et al.*, "Pilot-scale biomass gasification system for hydrogen production from palm kernel shell (part B): dynamic and control studies," *Biomass Convers. Biorefinery*, pp. 1-23, Jul. 2021, doi: 10.1007/S13399-021-01733-1/TABLES/10.

[41] K. A. Tran *et al.*, "Experimental and Computational Fluid Dynamics Investigation of

Rice Husk Updraft Gasifier with Various Gasification Agents," *Chem. Eng. Trans.*, vol. 63, pp. 223-228, May 2018, doi: 10.3303/CET1863038.

[42] S. Usmani *et al*., "Simulation model of the characteristics of syngas from hardwood biomass for thermally integrated gasification using unisim design tool," *Energy 2020*, vol. 211, pp. 118658, Nov. 2020, doi: 10.1016/j.energy.2020.118658

[43] N. Puadian, J. Li, and S. Pang, "Analysis of Operation Parameters in a Dual Fluidized Bed Biomass Gasifier Integrated with a Biomass Rotary Dryer: Development and Application of a System Model," *Energies 2014,* vol. 7, no. 7, pp. 4342-4363, Jul. 2014, doi: 10.3390/EN7074342.

[44] W. X. Peng, "Estudio de gasificación de biomasa para producción de combustiles alternativos, " *Conference: XLI Semana Nacional de Energía Solar*, Oct. 2017, Acessed: https://www.researchgate.net/publication/344252180_ESTUDIO_DE_GASIFICACION_DE_BIOMASA_PARA_PRODUCCION_DE_COMBUSTIBLES_ALTERNATIVOS

[45] A. A. Kasani, A. Esmaeili, and A. Golzary, "Software tools for microalgae biorefineries: Cultivation, separation, conversion process integration, modeling, and optimization," *Algal Res.*, vol. 61, pp. 102597, Jan. 2022, doi: 10.1016/J.ALGAL.2021.102597.

[46] COCO, "COCO Help: Gibbs minimization reactor." 2011, Acessed: https://www.cocosimulator.org/index_help.php?page=COUS/gibbsreactor.htm

[47] A. Technology, "HYSYS® 2004.2" *Operations Guide*, pp. 41-46, Oct. 2005, Acessed: https://sites.ualberta.ca/CMENG/che312/F06ChE416/HysysDocs/AspenHYSYSOperationsGuide.pdf

[48] A. Gambarotta, M. Morini, and A. Zubani, "A non-stoichiometric equilibrium model for the simulation of the biomass gasification process," *Appl. Energy*, vol. 227, pp. 119-127, Oct. 2018, doi: 10.1016/J.APENERGY.2017.07.135.

[49] V. Marcantonio, E. Bocci, and D. Monarca, "Development of a Chemical Quasi-Equilibrium Model of Biomass Waste Gasification in a Fluidized-Bed Reactor by Using Aspen Plus," *Energies 2020,* vol. 13, no. 1, pp. 53, Dec. 2019, doi: 10.3390/EN13010053.

[50] M. A. Yazdanpanah Jahromi, K. Atashkari, and M. Kalteh, "Development of a high-temperature two-stage entrained flow gasifier model for the process of biomass

gasification and syngas formation," *Int. J. Energy Res.*, vol. 43, no. 11, pp. 5864-5878, Sep. 2019, doi: 10.1002/ER.4692.

[51] S. Banerjee, J. A. Tiarks, and S.-C. Kong, "Modeling biomass gasification system using multistep kinetics under various oxygen-steam conditions," *Environ. Prog. Sustain. Energy*, vol. 34, no. 4, pp. 1148-1155, 2015, doi: 10.1002/ep.12109.

[52] W. C. Yan *et al.*, "Model-based downdraft biomass gasifier operation and design for synthetic gas production," *J. Clean. Prod.*, vol. 178, pp. 476-493, Mar. 2018, doi: 10.1016/J.JCLEPRO.2018.01.009.

[53] C. C. Sreejith, C. Muraleedharan, and P. Arun, "Air-steam gasification of biomass in fluidized bed with CO_2 absorption: A kinetic model for performance prediction," *Fuel Process. Technol.*, vol. 130, no. C, pp. 197-207, Feb. 2015, doi: 10.1016/J.FUPROC.2014.09.040.

[54] M. Trninić *et al.*, "A mathematical model of biomass downdraft gasification with an integrated pyrolysis model," *Fuel*, vol. 265, pp. 116867, Apr. 2020, doi: 10.1016/J.FUEL.2019.116867.

[55] A. Demirbas, "Effect of Temperature on Pyrolysis Products from Biomass, " *Energy Sources, Part A*, vol. 29, no. 4, pp. 329-336, 2010, doi: 10.1080/009083190965794.

[56] M. U. Hanif *et al.*, "Effects of Pyrolysis Temperature on Product Yields and Energy Recovery from Co-Feeding of Cotton Gin Trash, Cow Manure, and Microalgae: A Simulation Study," *Plos One*, pp. 1-11, Apr. 2016, doi: 10.1371/journal.pone.0152230.

[57] T. M. Ismail *et al.*, "Coal and biomass co-pyrolysis in a fluidized-bed reactor: Numerical assessment of fuel type and blending conditions," *Fuel*, vol. 275, pp. 118004, Sep. 2020, doi: 10.1016/J.FUEL.2020.118004.

[58] D. Glushkov *et al.*, "Current Status of the Pyrolysis and Gasification Mechanism of Biomass," *Energies 2021,* vol. 14, no. 22, pp. 7541, Nov. 2021, doi: 10.3390/EN14227541.

[59] M. U. Hanif *et al.*, "Influence of Pyrolysis Temperature on Product Distribution and Characteristics of Anaerobic Sludge," *Energies 2020,* vol. 13, no. 1, pp. 79, Dec. 2019, doi: 10.3390/EN13010079.

[60] M. Hu *et al.*, "Syngas production by catalytic in-situ steam co-gasification of wet sewage sludge and pine sawdust," *Energy Convers. Manag.*, vol. 111, pp. 409-416, Mar. 2016,

doi: 10.1016/J.ENCONMAN.2015.12.064.

[61] N. Nipattummakul *et al.*, "Hydrogen and syngas production from sewage sludge via steam gasification," *Int. J. Hydrogen Energy*, vol. 35, no. 21, pp. 11738-11745, Nov. 2010, doi: 10.1016/J.IJHYDENE.2010.08.032.

[62] J. Wang *et al.*, "Hydrogen-rich gas production by steam gasification of municipal solid waste (MSW) using NiO supported on modified dolomite," *Int. J. Hydrogen Energy*, vol. 37, no. 8, pp. 6503-6510, Apr. 2012, doi: 10.1016/J.IJHYDENE.2012.01.070.

[63] S. Luo *et al.*, "Hydrogen-rich gas from catalytic steam gasification of biomass in a fixed bed reactor: Influence of temperature and steam on gasification performance," *Int. J. Hydrogen Energy*, vol. 34, no. 5, pp. 2191-2194, Mar. 2009, doi: 10.1016/J.IJHYDENE.2008.12.075.

[64] K. Rabea *et al.*, "An improved kinetic modelling of woody biomass gasification in a downdraft reactor based on the pyrolysis gas evolution," *Energy Convers. Manag.*, vol. 258, Apr. 2022, doi: 10.1016/J.ENCONMAN.2022.115495.

[65] P. Lv *et al.*, "Hydrogen-rich gas production from biomass air and oxygen/steam gasification in a downdraft gasifier," *Renew. Energy*, vol. 32, no. 13, pp. 2173-2185, Oct. 2007, doi: 10.1016/J.RENENE.2006.11.010.

[66] D. Wang, W. Yuan, and W. Ji, "Char and char-supported nickel catalysts for secondary syngas cleanup and conditioning," *Appl. Energy*, vol. 88, no. 5, pp. 1656-1663, Dec. 2010, doi: 10.1016/J.APENERGY.2010.11.041.

[67] M. Dogru *et al.*, "Gasification of hazelnut shells in a downdraft gasifier," *Energy*, vol. 27, no. 5, pp. 415-427, May 2002, doi: 10.1016/S0360-5442(01)00094-9.

[68] Q. Dang *et al.*, "Prediction and optimization of syngas production from a kinetic-based biomass gasification process model," *Fuel Process. Technol.*, vol. 212, pp. 106604, Feb. 2021, doi: 10.1016/J.FUPROC.2020.106604.

[69] B. A. Oni *et al.*, "Experimental investigation of steam-air gasification of Cymbopogon citratus using Ni/dolomite/CeO_2/K_2CO_3 as catalyst in a dual stage reactor for syngas and hydrogen production," *Energy*, vol. 237, pp. 121542, Jul. 2021, doi: 10.1016/J.ENERGY.2021.121542.

[70] M. Ajorloo *et al.*, "Recent advances in thermodynamic analysis of biomass gasification: A review on numerical modelling and simulation," *J. Energy Inst.*, vol. 102, pp. 395-

419, Jun. 2022, doi: 10.1016/J.JOEI.2022.05.003.

[71] A. Ibrahim, S. Veremieiev, and P. H. Gaskell, “An advanced, comprehensive thermochemical equilibrium model of a downdraft biomass gasifier,” *Renew. Energy*, vol. 194, pp. 912-925, Jul. 2022, doi: 10.1016/J.RENENE.2022.05.069.

[72] W. C. Yan *et al.*, “Model-based downdraft biomass gasifier operation and design for synthetic gas production,” *J. Clean. Prod.*, vol. 178, pp. 476-493, Mar. 2018, doi: 10.1016/J.JCLEPRO.2018.01.009.

[73] J. Yu and J. D. Smith, “Validation and application of a kinetic model for biomass gasification simulation and optimization in updraft gasifiers,” *Chem. Eng. Process. - Process Intensif.*, vol. 125, pp. 214-226, Mar. 2018, doi: 10.1016/J.CEP.2018.02.003.

[74] S. Ghorbani *et al.*, “Three-stage modelling and parametric analysis of a downdraft biomass gasifier,” *Int. J. Hydrogen Energy*, vol. 47, no. 33, pp. 14799-14822, Apr. 2022, doi: 10.1016/J.IJHYDENE.2022.03.012.

[75] U. Kakati *et al.*, “Sustainable utilization of bamboo through air-steam gasification in downdraft gasifier: Experimental and simulation approach,” *Energy*, vol. 252, Aug. 2022, doi: 10.1016/J.ENERGY.2022.124055.

[76] W. Tauqir, M. Zubair, and H. Nazir, “Parametric analysis of a steady state equilibrium-based biomass gasification model for syngas and biochar production and heat generation,” *Energy Convers. Manag.*, vol. 199, pp. 111954, Nov. 2019, doi: 10.1016/J.ENCONMAN.2019.111954.

[77] L. García *et al*., “Catalytic Steam Gasification of Pine Sawdust. Effect of Catalyst Weight/Biomass Flow Rate and Steam/Biomass Ratios on Gas Production and Composition,” *Energy and Fuels*, vol. 13, no. 4, pp. 851-859, Jul. 1999, doi: 10.1021/EF980250P.

[78] J. J. Hernández *et al*., “Effect of steam content in the air-steam flow on biomass entrained flow gasification,” *Fuel Process. Technol.*, vol. 99, pp. 43-55, Jul. 2012, doi: 10.1016/J.FUPROC.2012.01.030.

[79] W. Doherty, A. Reynolds, and D. Kennedy, “The effect of air preheating in a biomass CFB gasifier using ASPEN Plus simulation,” *Biomass and Bioenergy*, vol. 33, no. 9, pp. 1158-1167, Sep. 2009, doi: 10.1016/J.BIOMBIOE.2009.05.004.